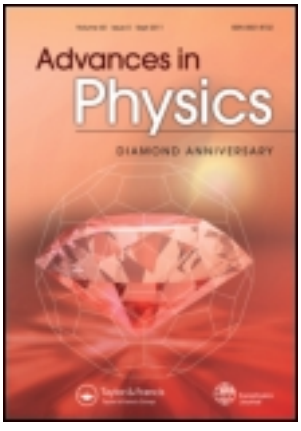

Advances in Physics
Publication details, including instructions for authors and subscription information:
http://www.tandfonline.com/loi/tadp20

Multichannel Kondo problem and some applications

P. Schlottmann [a] & P.D. Sacramento [b]

[a] Department of Physics , Florida State University , Tallahassee, Florida, 32306, USA

[b] Centro de Física da Matéria Condensada , 2 Av. Prof. Gama Pinto, 1699, Lisboa, Portugal

Published online: 28 Jul 2006.

To cite this article: P. Schlottmann & P.D. Sacramento (1993) Multichannel Kondo problem and some applications, Advances in Physics, 42:6, 641-682, DOI: 10.1080/00018739300101534

To link to this article: http://dx.doi.org/10.1080/00018739300101534

ADVANCES IN PHYSICS, 1993, VOL. 42, NO. 6, 641–682

Multichannel Kondo problem and some applications

By P. SCHLOTTMANN
Department of Physics, Florida State University
Tallahassee, Florida 32306, USA

and P. D. SACRAMENTO
Centro de Física da Matéria Condensada,
2 Av. Prof. Gama Pinto, 1699 Lisboa, Portugal

[Received 4 October 1993]

Abstract

We review analytical and numerical results derived from the Bethe ansatz solution of the n-channel Kondo model of arbitrary spin S as a function of temperature, external field, impurity spin S and the number of channels n. Three situations have to be distinguished: (i) If $n=2S$ the conduction electrons exactly compensate the impurity spin into a singlet at low temperatures, (ii) if $n<2S$ the impurity spin is only partially compensated (undercompensated), and (iii) if $n>2S$ the impurity spin is said to be overcompensated giving rise to critical behaviour. The results are discussed in the context of magnetic impurities, e.g. Fe, Cr and Tm in simple metals, the quadrupolar Kondo effect, an impurity spin embedded in the Takhtajan–Babujian Heisenberg model and electron assisted-tunnelling of an atom in a double-well potential.

Contents

	PAGE
1. Introduction	642
2. The n-channel Kondo problem. Model, Bethe-ansatz equations and numerical procedure	643
2.1. The model	643
2.2. Diagonalization of the model	644
2.3. Ground-state properties of the orbital singlet	646
2.4. Thermodynamics of the multichannel Kondo model	649
2.5. Thermodynamics: special limits and numerical procedure	650
3. The spin-compensated impurity case. Application to Fe and Cr impurities in simple metals	651
3.1. The model	651
3.2. Thermodynamic properties	652
3.3. The Kondo system Fe*Cu*	653
3.4. The Kondo system Fe*Ag*	655
3.5. The Kondo system Cr*Cu*	655
4. The undercompensated impurity spin case	657
4.1. Some analytic results	658
4.2. Some numerical results	658
5. The overcompensated impurity spin case	661
5.1. Some analytic results	661
5.2. Some numerical results	662
5.3. The quadrupolar Kondo effect	665
5.4. Electron assisted tunnelling of an atom in a double-well potential	667

0001–8732/93 $10·00

6. Heisenberg chain with impurity 671
6.1. Model and its diagonalization 671
6.2. Thermodynamic Bethe ansatz equations 673
6.3. Properties of the impurity 674
7. Concluding remarks 676
Acknowledgment 678
Appendix: Two-band model with attractive and repulsive interactions 678
References 679

1. Introduction

The exact solution of the Coqblin–Schrieffer model and the degenerate $U \to \infty$ Anderson model in terms of Bethe's ansatz opened the possibility of quantitative comparisons with experimental data for dilute Ce and Yb alloys [1], i.e. systems with *one* localized electron (hole) in the f shell. A remarkably good agreement was obtained for the temperature and field-dependence of the susceptibility, specific heat, magnetization and valence for the dilute systems Ce*Th*[1, 2], Ce*LaAl*$_2$ [1, 3] and Ce*LaB*$_6$ [1, 4], as well as for the compounds YbCuAl [1, 2, 5], $CeSn_3$ [1, 6], $YbCu_2Si_2$ [7] and $YbAgCu_4$ [8, 9] and the alloy system $Ce_{1-x}La_xPb_3$ [1, 10].

This analysis has been extended to the transition-metal impurities Fe and Cr in simple metals like Cu and Ag [11–13]. Realistic models for these impurities, as well as for Mn^{2+} and Eu^{2+} impurities, involve more than one localized electron (hole) and are necessarily more complex. The n-channel Kondo model [14, 15] provides a suitable description of such a system if one assumes that the orbital degrees of freedom are quenched by one or more mechanisms, leaving an orbital singlet. The low-temperature properties of such impurity systems are those of a totally compensated impurity spin (spin-singlet groundstate), which is achieved within the n-channel Kondo model if the number of channels is equal to $2S$ [15].

In general the number of channels and the impurity spin S can be considered as independent model parameters. Three qualitatively different situations have to be distinguished [15–17].

(i) If $n = 2S$ the number of conduction electron channels is exactly sufficient to compensate the impurity spin into a singlet, giving rise to Fermi-liquid behaviour.

(ii) If $n < 2S$ the impurity spin is only partially compensated (undercompensated spin), since there are not enough conduction electron channels to yield a singlet groundstate. This leaves an effective degeneracy (in zero field) at low temperatures of $(2S + 1 - n)$.

(iii) If $n > 2S$ the number of conduction-electron channels is larger than required to compensate the impurity spin. The impurity is said to be overcompensated and critical behaviour is obtained as the temperature and the external field tend to zero.

As mentioned above the compensated impurity spin case, $n = 2S$, is realized for effective S-state ions in simple metals, e.g. Fe*Cu*, Fe*Ag* and Cr*Cu* [11–13]. A possible application of the undercompensated situation could be the integer-valent limit of impurities with two magnetic configurations like Tm [1, 18]. Applications of the overcompensated case are the quadrupolar Kondo effect [19] and the electron assisted tunnelling of an atom in a double-well potential [20, 21]. A magnetic impurity embedded in the Takhtajan–Babujian generalization of the Heisenberg chain [22, 23]

has thermodynamic properties which are closely related to the three situations described above, depending on the relative magnitude of the lattice and impurity spins [24].

The purpose of this article is to review the diagonalization of the n-channel model via nested Bethe ansatze [16, 17, 25, 26] and the numerical solution of the resulting equations [27–29], as well as to discuss the above-mentioned applications and their physical relevance. In section 2 we introduce the model, the Bethe-ansatz equations and the numerical procedure to solve them. The spin compensated impurity case and its experimental relevance is discussed in section 3. Some results for the undercompensated situation are presented in section 4. The overcompensated situation and applications to the quadrupolar Kondo effect and electron assisted tunnelling of an atom in a double-well potential are discussed in section 5. In section 6 we summarize the relation between the n-channel Kondo problem and the Takhtajan–Babujian generalization of the Heisenberg chain with impurity. In the Appendix we briefly review the properties of an integrable one-dimensional two-band model of electrons involving attractive and repulsive interactions, that has a Bethe ansatz solution structurally very similar to the two-channel Kondo problem. Finally, some concluding remarks are given in section 7.

2. The n-channel Kondo problem. Model, Bethe-ansatz equations and numerical procedure

2.1. *The model*

The n-channel Kondo model for an impurity spin S and an arbitrary number of orbital conduction electron channels is given by [15]

$$H_K = \sum_{k,m,\sigma} \epsilon_k a^\dagger_{km\sigma} a_{km\sigma} + J \sum_{k,k',m,\sigma,\sigma'} \mathbf{S} \cdot a^\dagger_{km\sigma} \boldsymbol{\sigma}_{\sigma\sigma'} a_{k'm\sigma'}, \tag{2.1}$$

where $\mathbf{S}$ are the spin operators describing the magnetic impurity, J is the antiferromagnetic coupling constant, $\boldsymbol{\sigma}$ are the Pauli matrices and m labels the orbital channels. Although the Hamiltonian is diagonal in m the different orbital channels are not independent of each other. On the contrary, the exact solution [16, 17] shows that they are strongly correlated close to the impurity and form an orbital singlet, i.e., the spins of the conduction electrons at the impurity site are glued together to form a total spin $s_c = n/2$, which compensates the impurity degrees of freedom partially or totally.

In order to have an integrable model the kinetic energy of the electrons has to be linear in the momentum, i.e., all electrons move with Fermi velocity. A straight application of Bethe's ansatz then yields that the scattering matrix is diagonal in the orbital channel [16, 25, 30], i.e., proportional to $\delta_{m,m'}$. The spin and orbital channels, however, cannot be completely independent in a multiparticle process, since it would give rise to a degenerate groundstate of spin $S-1/2$, rather than a singlet [30]. The strong coupling between spin and orbital channels can be verified from the perturbative second-order corrections to the vertex function (or the invariant coupling) [15]. The $\delta_{m,m'}$ in the Bethe ansatz scattering matrix is an artifact of the linearization (and hence lack of energy cut-off) of the kinetic energy. Andrei and Destri [16] overcame this drawback by adopting an artificial cut-off procedure involving a quadratic term in the momentum, i.e., $\epsilon_k = k - k_F + \Lambda^{-1}(k-k_F)^2$. To preserve the integrability local counterterms must be added, which become irrelevant as $\Lambda \to \infty$. A similar cut-off scheme had been employed previously for the one-dimensional electron gas with backward scattering and linearized spectrum [31]. This regularization scheme applies to general S and arbitrary n.

Tsvelik and Wiegmann [17, 25, 32], on the other hand, considered an integrable variant of the Anderson model (see also [1]), which with the appropriate choice of parameters is equivalent to the exchange Hamiltonian (2.1),

$$H=\sum_{k,m,\sigma}(k-k_F)c^\dagger_{km\sigma}c_{km\sigma}+\epsilon_f\sum_{m,\sigma}f^\dagger_{m\sigma}f_{m\sigma}+V\sum_{k,m,\sigma}(c^\dagger_{km\sigma}f_{m\sigma}+f^\dagger_{m\sigma}c_{km\sigma})$$

$$-\tfrac{1}{2}U\sum_{m,m',\sigma,\sigma'}f^\dagger_{m\sigma}f^\dagger_{m'\sigma'}f_{m'\sigma}f_{m\sigma'}, \tag{2.2}$$

where ϵ_f is the f level energy, V is the hybridization between conduction and localized states, and $c^\dagger_{km\sigma}(f^\dagger_{m\sigma})$ creates a conduction electron (f electron) with orbital momentum m and spin σ (equation (2.2) is formulated in terms of f electrons (rare-earth or actinide impurities), but the same Hamiltonian also holds for transition metal impurities (d electrons)). The last term is not quite the standard Coulomb repulsion: For $U>0$ it represents an attraction within the orbital channel and a repulsion in spin space. Hence, this term tends to maximize the total spin of the shell, in accordance with the first Hund rule. For sufficiently large U and $0<\frac{1}{2}U(n-1)<\epsilon_f<\frac{1}{2}U(n+2)$, the ground-state of the shell is the orbital singlet, i.e., $L=0$, $S=n/2$. Note that this variant only corresponds to the spin compensated situation of the exchange model (2.1). We discuss this model in more detail below.

Tsvelik and Wiegmann [17, 32] also discovered an alternative exchange model leading to the same Bethe ansatz solution as model (2.1) in which electrons of spin $n/2$ (s_e) interact with an impurity of spin S_i,

$$H=\sum_{k,s}(k-k_F)c^\dagger_{ks}c_{ks}+\sum_{k,k',s,s'}c^\dagger_{ks}[P(\mathbf{S}_i\cdot\mathbf{s}_e)]_{s,s'}c_{k's'}, \tag{2.3}$$

where $P(x)$ is a polynomial of order $\min(2s_e, 2S_i)$ defined via the scattering matrix

$$S(x)=\exp[iP(x)]=-\sum_{|S_i-s_e|}^{S_i+s_e}\prod_{k=0}^{l}\frac{1-ikJ}{1+ikJ}\prod_{\substack{p=0\\p\neq l}}^{\min(2s_e,2S_i)}\frac{x-x_p}{x_l-x_p},$$

$$x_p=\tfrac{1}{2}p(p+1)-\tfrac{1}{2}S_i(S_i+1)-\tfrac{1}{2}s_e(s_e+1). \tag{2.4}$$

Here J is the coupling constant, assumed to be small ($\arctan(J)\approx J$). The Hamiltonian (2.3) is SU(2) invariant by construction and is closely related to integrable generalizations of the Heisenberg chain (Takhtajan–Babujian model [22, 23, 33, 34]). This model is defined for arbitrary n and S_i.

2.2. *Diagonalization of the model*

Although restricted to the situation $n=2S$, it is most instructive to diagonalize model (2.2) following the procedure outlined by Tsvelik and Wiegmann [17, 25], rather than the other two Hamiltonians. First the one- and two-particle problems are solved and then it is shown that the N-particle scattering matrix satisfies the factorization condition. The one-electron wavefunction consists of a plane wave propagating through the crystal with a phase-shift discontinuity at the impurity site of $2\phi_k$

$$\phi_k=\arctan[-\tfrac{1}{2}V^2/(k-\epsilon_f)], \tag{2.5}$$

where k is the momentum (and the energy) of the electron (see also [1]). The interaction U of course does not play any role in this case.

The ansatz for the two-particle wavefunction consists of terms corresponding to two propagating electrons of amplitude $g(x_1, x_2)$, one localized and one propagating electron, and two localized particles [1]. The function $g(x_1, x_2)$ has spin and orbital indices. The wavefunction is discontinuous along the lines $x_1 = 0$ and $x_2 = 0$, where one-body phase-shifts take place, and the derivative of the wavefunction has a jump along the line $x_1 = x_2$. The latter one has no physical implications, since $x_1 - x_2$ is a constant of motion, because all particles move with Fermi velocity. Without loss of generality we may factorize the amplitude $g(x_1, x_2)$ into a function depending only on the coordinates, a spin wavefunction and an orbital wavefunction. The total wavefunction is antisymmetric. For the spin and orbital parts we may use combinations of well-defined parity, i.e., singlet and triplet wavefunctions. If we choose both to have the same parity, then the coordinate-wavefunction must be antisymmetric and vanishes along the line $x_1 = x_2$. The discontinuity of the derivative of the wavefunction is trivially satisfied if the wavefunction vanishes along $x_1 = x_2$. To obtain a non-trivial solution, then, the spin and orbital functions must have different parity, so that the coordinate wavefunction is symmetric and non-vanishing if $x_1 = x_2$.

Assume the pair of electrons is in an orbital triplet state; then the spin wavefunction corresponds to the singlet. According to the Hamiltonian (2.2) the Coulomb interaction U is repulsive in this case. The scattering matrix is then the same as for the ordinary Anderson model [35] and does not depend on orbital indices. On the other hand, if the pair of electrons is in the orbital singlet (and hence in a spin triplet state) the interaction U is attractive and the scattering matrix does not depend on spin indices. The scattering matrix that combines all cases is given by [17, 25]

$$\hat{\mathbf{S}}(k_1 - k_2) = \hat{\mathbf{S}}_\sigma(k_1 - k_2) \otimes \hat{\mathbf{S}}_m(k_1 - k_2), \tag{2.6}$$

where in the limit $U \to \infty$ (see also [36])

$$\hat{\mathbf{S}}_\sigma(k_1 - k_2) = [(k_1 - k_2)\hat{I}_\sigma - \mathrm{i}V^2 \hat{P}_\sigma]/(k_1 - k_2 - \mathrm{i}V^2), \tag{2.7 a}$$

and

$$\hat{\mathbf{S}}_m(k_1 - k_2) = [(k_1 - k_2)\hat{I}_m + \mathrm{i}V^2 \hat{P}_m]/(k_1 - k_2 + \mathrm{i}V^2). \tag{2.7 b}$$

Here $\hat{I}_\sigma$, $\hat{I}_m$, $\hat{P}_\sigma$ and $\hat{P}_m$ are the identity and permutation operators for the spin and orbital indices, respectively. Note that equations (2.7) act as the identity on a triplet state, and for a product of singlet states the two phases cancel. Each of (2.7) separately obey the triangular Yang–Baxter relation [37], i.e., the many-particle scattering matrix can be factorized as a product of two-particle scattering matrices. Since they act in different spaces (spin and orbital), their product also satisfies the condition for the integrability of the model (2.2). Hence, every eigenstate of Hamiltonian (2.2) can be constructed from the general two-particle scattering matrix. The energy of the system is given by the sum over the momenta k_i.

So far the set of rapidities $\{k_j\}$ is arbitrary, except for the condition that the momenta are all unequal. The spectrum of the system with N particles is determined by imposing periodic boundary conditions on the wavefunction for each coordinate $k_j, j = 1, \ldots, N$. When one coordinate x_j is shifted to $x_j + L$, where L is the length of the box, the particle at x_j has to pass all other particles and also the impurity. Passing a particle means that the sequence of two coordinates is changed, involving in this way a two-particle scattering matrix. In addition, when the particle passes the impurity the phases of the amplitudes change according to the one-particle phase-shifts, (2.5). The

cyclic permutation of particle j yields an operator consisting of a product of N two-particle scattering matrices times a one-particle phase-shift. Periodic boundary conditions then give rise to an eigenvalue problem of N such operators, which is solved by a sequence of nested generalized Bethe ansatze [38]. Each ansatz eliminates one spin or orbital degree of freedom, so that there are altogether $2n$ ansatze, each one generating one additional set of rapidities. These sets are not independent but related via the discrete Bethe-ansatz equations [17, 25] (see also [1])

$$\exp[\mathrm{i}(k_j L+2\phi_j)]=\left(\prod_{\alpha=1}^{M} e[k_j-\lambda_\alpha]\right)\Big/\left(\prod_{\alpha=1}^{m_1} e[k_j-\xi_\alpha^{(1)}]\right),$$

$$\prod_{j=1}^{N} e[\lambda_\alpha-k_j]=-\prod_{\beta=1}^{M} e[(\lambda_\alpha-\lambda_\beta)/2],$$

$$\prod_{\beta=1}^{m_{l-1}} e[\xi_\alpha^{(l)}-\xi_\beta^{(l-1)}]\prod_{\beta=1}^{m_{l+1}} e[\xi_\alpha^{(l)}-\xi_\beta^{(l+1)}]=-\prod_{\beta=1}^{m_l} e[(\xi_\alpha^{(l)}-\xi_\beta^{(l)})/2], \tag{2.8}$$

where $j=1,\ldots,N$, $m_0=N$, $m_n=0$, $l=0,\ldots,n-1$, $\alpha=1,\ldots,m_l$, $\xi_j^{(0)}=k_j$ and $e[x]=(\mathrm{i}x+V^2/2)/(\mathrm{i}x-V^2/2)$. The only impurity contribution in (2.8) is the one-body phase-shift ϕ_j. All other factors are a parametrization of the free electron gas with two spin and n orbital degrees of freedom. The number of electrons with orbital quantum number l is $n_l=m_{l-1}-m_l$. The energy is given by $E=\Sigma_{j=1}^{N}k_j$, the total spin projection is $S_z=\frac{1}{2}N-M$ and the total orbital projection is $L_z=\frac{1}{2}N(n-1)-\Sigma_{j=1}^{n-1}m_j$.

2.3. *Ground-state properties of the orbital singlet*

In the orbital singlet state the number of electrons with orbital quantum number l is independent of l, $n_l=N/n$. We search for the orbital singlet ground-state, which is determined by the self-consistent solution of (2.8) with lowest energy and given spin magnetization S_z. The rapidities have in general complex values and for the ground-state in the thermodynamic limit they can be classified according to [17, 25, 32]

(i) there are $2S_z$ real charge rapidities k, which correspond to unpaired propagating electrons;
(ii) all other k's are complex and related to the λ's via $k^{\pm}=\lambda\pm\mathrm{i}\frac{1}{2}V^2$ (all λ's are real), corresponding to bound-states of electrons with opposite spin components;
(iii) there are $[(n-l)/n]2S_z$ real $\xi^{(l)}$ rapidities, $l=1,\ldots,n-1$, and,
(iv) $M(n-l)/2n$ strings of length 2 (bound pairs) of the form $\xi^{(l)}=\Lambda^{(l)}\pm\mathrm{i}\frac{1}{2}V^2$, where $\Lambda^{(l)}$ is a real parameter.

The fact that some $\xi^{(l)}$ are complex in the ground-state is due to the coupling of spin and orbital channels and the constraint of orbital singlet. If $S_z=N/2$, all the electrons have the same spin and $M=0$, such that all $\xi^{(l)}$ are real, in agreement with Sutherland's results [38] for the n-colour fermion gas in one dimension (repulsive δ-function interaction). On the other hand, if $S_z=0$, all orbital rapidities are complex, building bound pairs as a consequence of the orbital singlet restriction.

The above solutions of the discrete Bethe ansatz equations are inserted into equations (2.2) and the resulting expressions are made logarithmic. The logarithms give rise to sets of integers, which play the role of quantum numbers characterizing the state. For each set of real rapidities, i.e., $\{k_j\}$, $\{\lambda_\alpha\}$, $\{\xi_\alpha^{(l)}\}$ and $\{\Lambda_\alpha^{(l)}\}$, $l=1,\ldots,n-1$, a corresponding set of quantum numbers is obtained. In the ground-state each set of

quantum numbers forms a string of consecutive integers and all quantum numbers within a set are different. As a consequence of the orbital singlet condition, in the thermodynamic limit ($L\to\infty$, $N\to\infty$, $M\to\infty$ with N/L and M/L kept constant) the rapidities $\xi^{(l)}$ and $\Lambda^{(l)}$ take values filling the entire real axis, while the λ's are confined to the interval $(-\infty, Q)$ and the k's to $(-\infty, B)$. The rapidities $\xi^{(l)}$ and $\Lambda^{(l)}$ are then not affected by changes of physical parameters, and can be eliminated from the problem by means of a series of algebraic operations. It is convenient to introduce distribution functions for the rapidities λ and k, $\sigma(\lambda)$ and $\rho(k)$, and similarly the corresponding 'hole' distributions, $\sigma_h(\lambda)$ and $\rho_h(k)$. Differentiating with respect to the rapidity and in the thermodynamic limit, we then obtain, after Fourier transforming and some algebra, two coupled linear integral equations of the Wiener–Hopf type for the distribution densities, i.e., [17]

$$\begin{aligned}\rho_h(k)+&\int_{-\infty}^{B}d\xi\,\rho(\xi)\int_{-\infty}^{\infty}\frac{dx}{2\pi}\exp[-ix(\xi-k)+\tfrac{1}{2}(n-1)V^2|x|]\frac{\sinh(V^2x/2)}{\sinh(nV^2x/2)}\\&+\int_{-\infty}^{Q}d\xi\,\sigma(\xi)\int_{-\infty}^{\infty}\frac{dx}{2\pi}\exp[-ix(\xi-k)+\tfrac{1}{2}(n-2)V^2|x|]\frac{\sinh(V^2x/2)}{\sinh(nV^2x/2)}\\&=\frac{1}{2\pi}+\frac{1}{\pi L}\frac{V^2/2}{(k-\epsilon_f)^2+(V^2/2)^2},\end{aligned}\tag{2.9}$$

$$\begin{aligned}\sigma_h(\lambda)+&\int_{-\infty}^{Q}d\xi\,\sigma(\xi)\int_{-\infty}^{\infty}\frac{dx}{2\pi}\exp[-ix(\xi-\lambda)+\tfrac{1}{2}(n-2)V^2|x|]\frac{\sinh(V^2x)}{\sinh(nV^2x/2)}\\&+\int_{-\infty}^{B}d\xi\,\rho(\xi)\int_{-\infty}^{\infty}\frac{dx}{2\pi}\exp[-ix(\xi-\lambda)+\tfrac{1}{2}(n-2)V^2|x|]\frac{\sinh(V^2x/2)}{\sinh(nV^2x/2)}\\&=\frac{1}{\pi}+\frac{1}{\pi L}\frac{V^2}{(\lambda-\epsilon_f)^2+V^4}.\end{aligned}\tag{2.10}$$

The right-hand sides of equations (2.9) and (2.10) represent the driving terms of the integral equations. The distribution functions $\rho(k)$ and $\sigma(\lambda)$ can be separated into two terms, a host (electron gas) contribution (independent of L) and an impurity part, which arises from the $1/L$ driving terms. The energy, the magnetization and the number of electrons are given by

$$\begin{aligned}E/L&=\int_{-\infty}^{B}dk\,k\,\rho(k)+2\int_{-\infty}^{Q}d\lambda\,\lambda\,\sigma(\lambda),\\S_z/L&=\frac{1}{2}\int_{-\infty}^{B}dk\,\rho(k),\qquad L_z=0,\\N/L&=\int_{-\infty}^{B}dk\,\rho(k)+2\int_{-\infty}^{Q}d\lambda\,\sigma(\lambda).\end{aligned}\tag{2.11}$$

The two integration limits B and Q are determined by the magnetization and the total number of electrons.

We first obtain the valence of the impurity in model (2.2) as a function of the f-level energy ϵ_f. In the absence of a magnetic field, the magnetization vanishes such that

$B=-\infty$. This reduces equation (2.10) to a single Wiener-Hopf integral equation for the density $\sigma(\lambda)$. Its solution is standard and we obtain [1, 26]

$$n_f = 2\int_{-\infty}^{Q} d\lambda\, \sigma_{imp}(\lambda)$$
$$= n\left[1+i\int_{-\infty}^{\infty}\frac{dx\exp(ic^*x)}{2\pi}\frac{}{x-i0}\left(\frac{ix+0}{e}\right)^{ix}\left(\frac{-ix+0}{e}\right)^{-inx/2}\frac{\Gamma(1-ix)}{\Gamma(1-\frac{1}{2}inx)}\right], \tag{2.12}$$

where $\epsilon^*=(\pi/V^2)(\epsilon_f-Q)-\frac{1}{2}n\ln(\frac{1}{2}n)$ is a renormalized f-level energy and Γ denotes the gamma function. As a function of ϵ^*, n_f varies smoothly between 0 ($\epsilon^*\to+\infty$) and n ($\epsilon^*\to-\infty$). This range is determined by the $U\to\infty$ limit taken before. Consequently (2.12) is physically meaningful only for $\epsilon^*\ll 0$, where it approaches the half-filled shell occupation as

$$n_f/n = 1-1/|\epsilon^*|+\tfrac{1}{2}(n-2)\ln|\epsilon^*|/|\epsilon^*|^2+\ldots. \tag{2.13}$$

Identifying $|\epsilon^*|\sim\ln(D/T_K)$, we recover the characteristic logarithmic dependence of the Kondo problem.

The zero-field susceptibility is obtained by eliminating $\sigma(\lambda)$ from equations (2.9) and (2.10). This leads to one Wiener–Hopf integral equation for $\rho(k)$ with two driving terms, one being the impurity Kondo term and the other one arising from the charge fluctuations (described by $\sigma_h(\lambda)$) in the electron gas and at the impurity. The feedback of the magnetic field H on $\sigma_h(\lambda)$ is of higher order than linear and can be neglected in linear response, i.e., the zero-field solution for $\sigma_h(\lambda)$ is used [1, 26, 39]. The solution of the Wiener–Hopf equation then yields

$$\chi_{imp}=\frac{\pi\exp[-\epsilon^*-(n-2)/2]}{2V^2\Gamma(n/2)}$$
$$-i\frac{n}{8V^2}\int_{-\infty}^{\infty}dx\frac{\exp(ixc^*)}{x-i}\frac{\Gamma(1-ix)}{\Gamma(1-\frac{1}{2}inx)}\left(\frac{ix+0}{e}\right)^{ix}\left(\frac{-ix+0}{e}\right)^{-inx/2}, \tag{2.14}$$

where the first term is the Kondo susceptibility and the second one is induced by the valence fluctuations. As the valence approaches the half-filled shell (as $\epsilon^*\to-\infty$) the Kondo term grows exponentially and the valence-induced spin fluctuations decrease as $(\epsilon^*)^{-2}$.

Finally we give the result for the magnetization as a function of field for the integer-valent limit. Charge fluctuations are suppressed as $Q\to\infty$ and hence $\sigma_h(\lambda)\equiv 0$. Eliminating $\sigma(\lambda)$ from (2.9) using (2.10) one obtains a Wiener–Hopf integral equation for $\rho(k)$. The solution of this equation yields the impurity magnetization [17, 25]

$$M=\frac{1}{2}\int_{-\infty}^{\infty}dk\,\rho(k)$$
$$=\frac{in}{4\pi^{3/2}}\int_{-\infty}^{\infty}dx\frac{\exp(i\tilde{\epsilon}x)}{x+i0}\left(\frac{-ix+0}{e}\right)^{-inx/2}\frac{\Gamma(\frac{1}{2}+\frac{1}{2}ix)\Gamma(1-\frac{1}{2}ix)}{\Gamma(1-\frac{1}{2}inx)}, \tag{2.15}$$

where $\tilde{\epsilon}$ is the dimensionless parameter $\tilde{\epsilon}=(\pi/V^2)(\epsilon_f-B)-\frac{1}{2}n\ln(\frac{1}{2}n)$. For a small magnetic field we obtain

$$M=\exp(-\tilde{\epsilon}-\tfrac{1}{2}n)/\Gamma(\tfrac{1}{2}n)=\chi_{imp}H,$$

so that using (2.14) we can identify $B-Q=(V^2/\pi)\ln(\pi eH/2V^2)$. For large fields, on the other hand, we have

$$M=\tfrac{1}{2}n[1-n/(2|\tilde{\epsilon}|)-(n/2\tilde{\epsilon})^2\ln|\tilde{\epsilon}|+\ldots]. \tag{2.16}$$

Defining $T_K=(n/2\pi\chi_{imp})$ in the integer-valent limit of (2.14), we have that $\tilde{\epsilon}\sim\ln(T_K/H)$ and that the magnetization is a universal function of H/T_K, which shows the characteristic Kondo logarithms in the high-field limit.

2.4. *Thermodynamics of the multichannel Kondo model*

The partition function can be obtained if all excitation energies or their distribution densities are known. This is quite tedious for model (2.2), which involves all orbital, spin and charge degrees of freedom (see [26]). A simplifying shortcut is possible, if we restrict ourselves to the orbital singlet and the Kondo limit, i.e., spin excitations only. In the limit $Q\to\infty$ the charge excitations are suppressed (i.e., $\sigma_h(\lambda)\equiv 0$) and equations (2.9) and (2.10) reduce to a single integral equation for ρ, which can be written as [1]

$$\rho(\lambda)+\rho_h(\lambda)+\sum_{l=1}^{n}(2-\delta_{l,n})\frac{1}{\pi}\frac{lV^2}{\lambda^2+(lV^2)^2}*\rho_h(\lambda)=\sum_{l=1}^{n}\frac{1}{\pi}\frac{(l-\frac{1}{2})V^2}{(\lambda-\epsilon_f)^2+[(l-\frac{1}{2})V^2]^2}, \tag{2.17}$$

where * denotes a convolution. Consider now the following set of discrete equations ($\alpha=1,\ldots,M$):

$$e[(\xi_\alpha-\epsilon_f)/n][e(\xi_\alpha/n)]^N=\prod_{\beta=1}^{M}e[(\xi_\alpha-\xi_\beta)/2], \tag{2.18}$$

where the first factor on the left-hand side represents the impurity. In the thermodynamic limit the solutions to (2.18) are strings of arbitrary length l,

$$\xi_{\alpha,l}^{\mu}=\lambda_\alpha^{(l)}+\tfrac{1}{2}iV^2(l+1-2\mu), \qquad \mu=1,\ldots,l. \tag{2.19}$$

Assuming that the ground-state consists of strings of length n only (i.e., n spin-flips glued together in a bound-state to form a spin $s_e=n/2$, necessary to compensate the impurity spin $S=n/2$), then inserting them into (2.18) and logarithmizing the equations, we obtain (2.17) for the impurity part of (2.19). With this argument it is plausible that (2.18) is closely related to the multichannel Kondo problem [17]. Indeed, (2.18) combined with

$$\exp(ik_jL)=\prod_{\alpha=1}^{M}e(\xi_\alpha/n), \qquad j=1,\ldots,N, \tag{2.20}$$

are just the discrete Bethe ansatz equations for the alternative model (2.3), where N is the number of electrons, $S_z=\frac{1}{2}N-M$ is the magnetization and the energy is given by $E=\Sigma_{j=1}^{N}k_j$. A proof of the equivalence of model (2.3) to the multichannel Kondo problem can be found in [32].

We proceed to obtain the thermodynamics of model (2.3). All excitations are characterized by real rapidities k and the strings (2.19). Inserting the strings into (2.18), logarithmizing the resulting equations and differentiating them with respect to λ we obtain (after some algebra) the spectral equations relating particles and holes (i.e., the Fermi statistics obeyed by the rapidities) [32]

$$2\cosh(\tfrac{1}{2}V^2x)[\hat{\rho}_l(x)+\hat{\rho}_{l,h}(x)]=\hat{\rho}_{l+1,h}(x)+\hat{\rho}_{l-1,h}(x)+\delta_{l,n}\left[\frac{N}{L}+\frac{1}{L}\exp(i\epsilon x)\right], \tag{2.21}$$

where ρ_l is the distribution density for the real $\lambda_\alpha^{(l)}$, $\rho_{l,h}$ is the corresponding 'hole' distribution and the *hat* denotes Fourier-transform. Here ρ_0 and $\rho_{0,h}$ are identically zero. The spectral relations are valid without restriction in the thermodynamic limit.

We impose thermal equilibrium by minimizing the free energy functional, $F=E-TS$, with respect to the particle and hole density functions, subject to the constraints (2.21) and a constant magnetization, $S_z/L=N/2L-\Sigma_{l=1}^{\infty} l\int\rho_l(\lambda)\,d\lambda$. The energy functional is obtained via (2.20),

$$E/L=\text{const.}+\frac{N}{2\pi L}\int_{-\infty}^{\infty} d\lambda\left\{\frac{\pi}{2}+\arctan\left[\exp(\pi\lambda/V^2)\right]\right\}\rho_{n,h}(\lambda), \tag{2.22}$$

and the entropy is given by the Fermi statistics of the rapidities. The minimization of the free energy finally yields the following infinite recursion sequence (setting $V^2=2\Gamma=2$)

$$\ln\left[\eta_l(\lambda)\right]=G^*\ln\left[(1+\eta_{l-1})(1+\eta_{l+1})\right]-\delta_{l,n}\exp(\pi\lambda/2), \tag{2.23}$$

where $\eta_0\equiv 0$, $\eta_l=\rho_{l,h}/\rho_l$, the integration kernel is defined $G(\lambda)=[4\cosh(\pi\lambda/2)]^{-1}$ and $\lambda\to\lambda-(2/\pi)\ln(\epsilon_F/T)$ with ϵ_F being the Fermi energy. These equations are completed by the asymptotic condition

$$\lim_{l\to\infty}(1/l)\ln\left[\eta_l(\lambda)\right]=H/T=2x_0, \tag{2.24}$$

and the impurity contribution to the free energy (up to an additive constant) is given by

$$F=-T\int_{-\infty}^{\infty} d\lambda\, G[\lambda-(2/\pi)\ln(T_K/T)]\ln\left[1+\eta_{2S}(\lambda)\right], \qquad n=2S, \tag{2.25}$$

where $T_K\sim\epsilon_F\exp(\pi\epsilon_f/V^2)$ is the Kondo temperature [16, 26]. Note that the field and temperature dependence of the equations only enters via the asymptotic condition (2.24). For $H=0$ the properties of the impurity are then universal as a function of T/T_K. For $n=1$ the spin 1/2 Kondo problem [40] is recovered and except for the driving term in (2.23) the integral equations for arbitrary n are the same as for the SU(2)-invariant Heisenberg chain of spin $S=n/2$ (Babujian–Takhtajan model) [23, 41].

Finally, the thermodynamic Bethe ansatz equations corresponding to the extension of these results to $n\neq 2S$ are still (2.23) through (2.25), but with $2S\neq n$ in (2.25) [16, 26].

2.5. *Thermodynamics: special limits and numerical procedure*

In the limits $\lambda\to\pm\infty$ the λ dependence in (2.23) becomes irrelevant and the equations can be solved analytically. The asymptotic solutions are [27]

$$\ln\left[1+\eta_l(+\infty)\right]=\begin{cases}2\ln\{\sin[\pi(l+1)/(n+2)]/\sin[\pi/(n+2)]\}, & l<n,\\ 2\ln\{\sinh[(l+1-n)x_0]/\sinh(x_0)\}, & l\geqslant n,\end{cases}$$

$$\ln\left[1+\eta_l(-\infty)\right]=2\ln\{\sinh[(l+1)x_0]/\sinh(x_0)\}, \qquad \forall l.$$

The functions $\eta_l(\lambda)$ are monotonically decreasing functions of λ and interpolate smoothly between the asymptotic values at $\lambda\to\pm\infty$. The limit $\lambda\to-\infty$ corresponds to the high-temperature regime, while $\lambda\to+\infty$ represents the low-temperature limit. From the above equations it is clear that the η_l are finite and non-zero everywhere, except for $l=n$ as λ tends to $+\infty$, where η_n tends to zero. Hence, the conduction electron states coupling to the impurity at low T consist of bound states of n spin waves,

i.e., n spin waves are strongly coupled in orbital singlet states of effective spin $s_e = n/2$. All other states are frozen out or decoupled from the impurity at low T.

For intermediate values of λ the recursion sequence (2.23) has to be solved numerically. To implement this solution the infinite sequence (2.23) is truncated at an index l_c and the functions $\ln(1+\eta_l)$ for $l > l_c$ are replaced by an appropriate interpolating asymptotical form. The numerical problem then reduces to the simultaneous solution of l_c coupled integral equations. Also the range of values of λ is truncated at $\pm\lambda_c$ where λ_c is a value of the rapidity so that all the functions $\eta_l(\lambda)$ have reached their asymptotic values. The errors in the free-energy derivatives (obtained numerically) are controlled by varying l_c and λ_c. Satisfactory results for $2x_0 = H/T < 10$ were obtained for $l_c = 50$ and $\lambda_c = 56$ [11, 28, 29, 42]. This method is similar to the ones employed elsewhere [1, 3, 27], except that a higher numerical precision is required if $n \neq 2S$, in particular if $n > 2S$.

This numerical procedure is not accurate enough at low temperatures for $H/T > 10$ and the numerical derivatives turn out to be unreliable. This is in part due to the exponential behaviour with x_0 of the above asymptotic expressions, but arises mainly from the exponential dependence on λ of the integration kernel and the asymptotic of the function η_l for $l \leqslant n$. The low-T properties of the impurity are determined by the $\lambda \to +\infty$ asymptotic of η_{2S}. This low-T behaviour is particularly difficult to obtain in the overcompensated case. A brief description of the procedure employed for $H/T > 10$ can be found in [28] (for a detailed outline see [27, 43]).

In summary, we solve the thermodynamic Bethe ansatz equations using two different numerical procedures: a standard one giving good results for $H/T < 10$ and a second one suitable for $H/T > 10$. The results for C/T (second temperature derivative of the free energy) match at $H/T = 10$ within a few per cent.

3. The spin-compensated impurity case
Application to Fe and Cr impurities in simple metals

In this section we discuss the physical properties of the spin-compensated situation $n = 2S$ and its applications to three experimental systems, namely Fe*Cu*, Fe*Ag* and Cr*Cu*.

3.1. *The model*

The commonly accepted basic model describing the interaction of a magnetic impurity with a metallic host is the orbitally degenerate Anderson model, which in the integer-valent limit reduces (via a Schrieffer–Wolff transformation) to an exchange Hamiltonian involving spin and orbital indices [14, 15, 44]. The ground-state of such a system is believed to be a singlet, giving rise to a finite susceptibility and a specific heat proportional to temperature.

Iron and chromium have several electrons in their 3d shell and according to the first Hund's rule their spins in the ground-multiplet are coupled into a manifold characterized by a spin S. The exchange Hamiltonian projected onto the impurity state of spin S is given by

$$H_{ex}^{(S)} = \frac{J}{S} \sum_{\substack{k,k',m,m' \\ M,M',\sigma,\sigma'}} b_{mM}^{\dagger} \mathbf{S}_{MM'} b_{m'M'} \cdot c_{k'm'\sigma'}^{\dagger} \mathbf{s}_{\sigma'\sigma} c_{km\sigma}, \tag{3.1}$$

where $b_{mM}^{\dagger}$ creates a localized electron with orbital momentum (l, m) in the state of total spin (S, M). Hamiltonian (3.1) is not diagonal in the indices m and m' and hence different

from the standard n-channel model. Here the orbital channel is not restricted to a singlet, but to all allowed total orbital angular momentum values L.

There are several competing interactions next in the hierarchy of energy scales, all restricting the orbital degrees of freedom, namely (i) Hund's second rule maximizing the orbital angular momentum, (ii) cubic crystalline fields quenching the orbital angular momentum and (iii) the rather large hybridization width of the 3d levels smearing the energy splitting of the ionic terms. The spin–orbit coupling is somewhat smaller than the above energies. It is difficult to predict the effect of the interplay and combined action of these energy scales, but to reduce the dynamics within the orbital channel. A further mechanism that would lead to an orbital singlet is the orbital exchange [44]; the screening of the orbital degrees of freedom is expected to occur at an energy much higher than the Kondo temperature.

Experiments indicate that the Fe*Cu*, Fe*Ag* and Cr*Cu* systems are a spin singlet at low temperatures. The simplest model involving several localized electrons yielding a finite magnetic susceptibility is the n-channel Kondo model with $n=2S$, given by Hamiltonian (3.1) with the restriction $m=m'$ arising from the orbital singlet condition [15]. Below we discuss the physical properties of the completely compensated situation and compare these results to experiments. There are two parameters to be adjusted, T_K and n, the effective number of channels. The best fit for n is not necessarily five, as expected for d electrons, but can be smaller. A possible interpretation of an 'effective' $n\neq 5$ is that only those orbital channels that are actually represented in the local moment at a given instant can participate in the scattering.

3.2. *Thermodynamic properties*

We first discuss the low- and high-temperature solutions of the thermodynamic equations. It is convenient to define energy potentials for the string excitations

$$\epsilon_l(\lambda)=T\ln\eta_l(\lambda). \tag{3.2}$$

As $T\to 0$ equations (2.23) reduce to (by reversing the shift of λ with $\lambda\to\lambda+(2/\pi)\ln(\epsilon_F/T)$)

$$\epsilon_l=G*(\epsilon_{l-1}^{+}+\epsilon_{l+1}^{+})-\delta_{l,n}\epsilon_F\exp(\pi\lambda/2),\qquad \epsilon_0^{+}\equiv 0, \tag{3.3}$$

where $\epsilon_l=\epsilon_l^{+}+\epsilon_l^{-}$, with $\epsilon_l^{+}>0$ and $\epsilon_l^{-}<0$ [1, 26]. It follows that $\epsilon_l^{-}\equiv 0$ for all l except for $l=n$ and hence $\rho_l\equiv 0$ for $l\neq n$. Only strings of length n exist in the ground state, confirming the conjecture in the previous section. This is consistent with n conduction electron spins glued together to compensate the impurity spin $S=n/2$. ϵ_n is a monotonically decreasing function of λ and we define B such that $\epsilon_n^{+}(B)=0$. Solving the Wiener–Hopf integral equation obeyed by ϵ_n we recover the ground-state properties already discussed in section 2.3.

For small but finite T the Fermi liquid properties can be extracted [16, 26]. Since the ground-state is a singlet, the specific heat is proportional to T, and γ can be obtained via a Sommerfeld expansion [34],

$$\gamma=\pi n/[(n+2)T_K]. \tag{3.4}$$

Combined with the zero-field susceptibility ($\chi_s=n/(2\pi T_K)$) we obtain the Wilson ratio for the impurity [15, 45, 46],

$$(\pi^2/3)(\chi_s/\gamma)=(n+2)/6. \tag{3.5}$$

For $n=1$ this result includes the Wilson ratio of the ordinary Kondo problem [47].

According to (2.25) the high-temperature free energy is determined by $\eta_n(-\infty)$. Since $\eta_n(-\infty)$ is independent of λ, the integration is straightforward and we have $(n=2S)$

$$F=-T\ln\{\sinh[(2S+1)H/2T]/\sinh(H/2T)\}. \tag{3.6}$$

This is the free energy of an isolated spin S; perturbative corrections are logarithmic, characteristic of asymptotic freedom.

To obtain the susceptibility and specific heat at arbitrary temperatures the integral equations (2.23) subject to the asymptotic condition (2.24) must be solved numerically, following the procedure described above in section 2.5. The ϵ_l form (overlapping for $n>1$) bands with a temperature-dependent dispersion; they are occupied according to Fermi statistics, i.e., a negative ϵ_l favours occupation of the state, while if ϵ_l is positive it tends to be empty.

The zero-field susceptibility as a function of temperature was obtained by Desgranges [27]. $\chi_n(T)$ scaled to its $T=0$ value, $\chi_n=n/(2\pi T_K)$, has the interesting feature that it is almost independent of n and only a function of T/T_K, i.e., it essentially scales with the spin-1/2 Kondo problem. The specific heat is linear in T at low T and has a maximum at about $T\sim T_K/2$. Again, if plotted as $C(T)/\gamma$ against T/T_K the maximum height of the peak and the low-T behaviour are only weakly dependent on n, but the dependence of the high-T asymptotic on n is stronger [27]. For $n>1$ the temperature dependence of both χ and C/T is qualitively different from the one displayed by the Coqblin–Schrieffer model [48] (i.e., a maximum as a function of T arising from the thermal population of the Kondo peak situated above the Fermi level) and decrease monotonically with T, indicating that the Kondo peak is on-resonance with the Fermi level, as a consequence of the electron-hole symmetry.

The low-temperature resistivity due to the impurity has been derived within a Fermi-liquid approach assuming electron–hole symmetry about the Fermi level [45, 46],

$$R_{\text{imp}}=R_0\{1-(1/8)[5\pi/(n+2)]^2(T/T_K)^2\}, \tag{3.7}$$

where R_0 corresponds to the scattering at the unitarity bound.

3.3. *The Kondo system Fe*Cu

Experiments indicate that the Fe*Cu* system is a magnetic singlet at low temperatures. We now compare exact results for the multichannel Kondo problem to data for Fe*Cu* [11], which is probably the best studied dilute transition metal alloy showing the Kondo effect.

As mentioned above $\chi_n(T)/\chi_n(0)$ is almost independent of n, so that by comparison with the experimental data (see figure 1 (*a*)) we obtain $T_K=18$ K. Two sets of data have been employed: (i) the bulk measurements of Tholence and Tournier (dark squares) [49], who analysed their data as a function of concentration to extrapolate the single impurity behaviour, and (ii) Mössbauer data by Steiner *et al.* (open squares) [50] taken at p.p.m. Fe concentrations. The agreement with the theory is better for the local susceptibility (Mössbauer) than for the bulk data.

The 'parameter' $n=2S$ can be determined from the experimental susceptibility extrapolated to zero temperature. $\chi_n(T=0)=ng^2/(2\pi T_K)$, for $T_K=18$ K and $g=2$ (orbital singlet) yields $n\,0{\cdot}237$ emu/g, which is to be compared to the experimental single-ion value obtained by Tholence and Tournier [49] of about 0·90 emu/g. The agreement is best if the effective n is 4, i.e., for a spin $S=2$. Iron is usually trivalent in

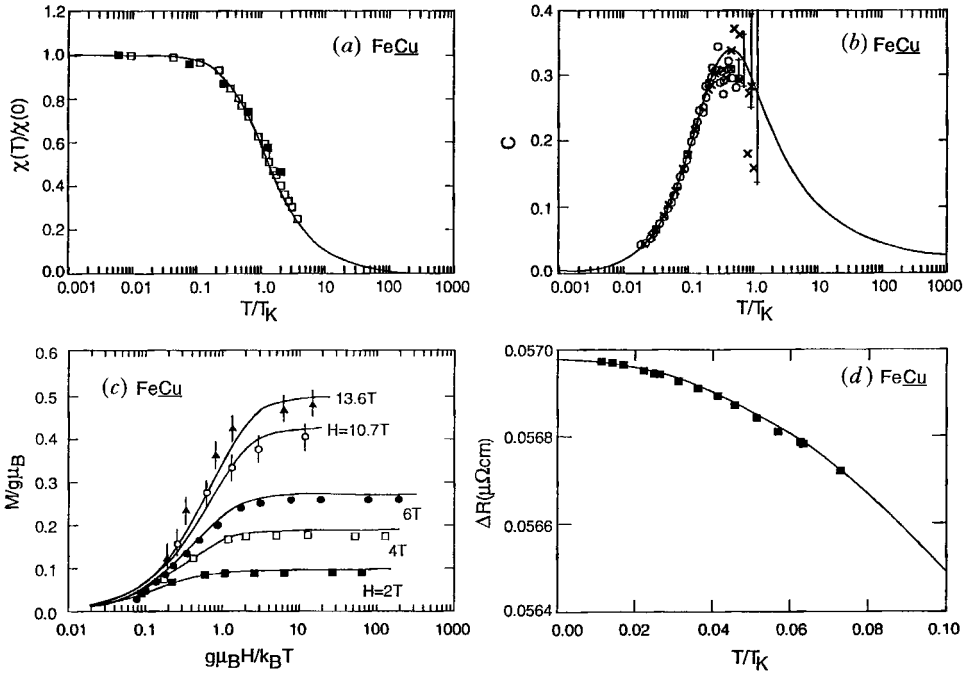

Figure 1. Comparison of theory for the $S=n/2$ multi-channel Kondo model with experimental data for dilute Fe*Cu* alloys [11]. (*a*) Zero-field susceptibility normalized to its $T=0$ value as a function of T for $T_K=18$ K (open squares: Mössbauer data of Steiner *et al.* [50]; dark squares: bulk-χ data by Tholence and Tournier [49]). (*b*) Specific heat per impurity in units of k_B as a function of T for $T_K=18$ K. The solid line is the $S=2$ curve, open circles correspond to 195 p.p.m. Fe data and crosses to measurements on a 81·4 p.p.m. Fe sample (from figure 3 of [52]). (*c*) Magnetization in units of $g\mu_B$ in constant field as a function of $(g\mu_B H/k_B T)$. The solid lines are the theoretical curves for $S=2$, $g=2$ and $T_K=18$ K. The field is in Tesla. The low field data ($H=2\,T$, $4\,T$ and $6\,T$) is from [53] and the high-field data ($H=10{\cdot}7\,T$ and $13{\cdot}6\,T$) from [54]. The magnetization data has been scaled with a hyperfine saturation field of $(-11{\cdot}1\pm0{\cdot}3)\,T$ [50]. (*d*) Low-temperature resistivity difference of a 50 p.p.m. Fe alloy and pure Cu as a function of T. The solid line is the Fermi-liquid expression, (3.7), and the data are from figures 3 and 4 of [55].

insulators, but is expected to be divalent in metals. Fe^{2+} has six electrons (four holes) in the 3d shell and hence the Hund's rule ground-state has total spin $S=2$.

Without further adjustable parameters we now compare the theory to the experimental data for the specific heat. The low T specific heat is proportional to T, the coefficient γ being determined by n and T_K, according to (3.4). The experimental zero-field data of Triplett and Phillips [51, 52] for samples of 81·4 p.p.m. and 195 p.p.m. Fe is found to be in good agreement with the theoretical curve for $n=4$ and $T_K=18$ K (see figure 1 (*b*)). The large error bars at the higher temperatures are due to the relatively large phonon contributions.

The magnetization as a function of field and temperature as measured via the Mössbauer effect is shown in figure 1 (*c*) together with the theoretical curves for $T_K=18$ K, $n=4$ and $g=2$. The agreement is remarkable, considering that there is no further adjustable parameter. Two sets of data are available: the more precise low field (up to 6 T) points were obtained by Steiner *et al.* [53], while the high field data are from Frankel *et al.* [54]. A hyperfine saturation field of $-11{\cdot}1\pm0{\cdot}3$ T has been used to scale the data [50].

The resistivity difference of that of an alloy with 50 p.p.m. Fe and pure Cu [55] is shown in figure 1 (*d*). R_0 is determined from the extrapolation to $T=0$ and the solid line represents (3.7) for $n=4$ and $T_K=18$ K.

3.4. *The Kondo system Fe*Ag

The Kondo system Fe*Ag* is expected to behave similarly to Fe*Cu*, i.e., we will use $n=4$ and $g=2$ (orbital singlet) for our analysis and keep the Kondo temperature as the adjustable parameter [13]. Unfortunately the experimental data on Fe*Ag* is very limited, i.e. restricted to susceptibility and magnetization, but no specific heat and resistivity measurements are available. The T_K for this alloy is 2 K, that is much smaller than for Fe*Cu*. A small T_K implies that also the exchange constant, J, is small and as a consequence the Ruderman–Kittel–Kasuya–Yosida (RKKY) interaction between impurities becomes relatively more important. As argued by Doniach [56], the RKKY interaction grows as J^2 with J, while T_K follows an exponential dependence, $T_K \sim D\exp(-1/J\rho)$. Due to the relative importance of impurity–impurity interactions, it is then necessary to experimentally study the ultra-dilute limit to investigate single-impurity properties. This seriously complicates specific heat and resistivity measurements, but ultra-dilute experiments for magnetic properties can be achieved via the Mössbauer effect (concentrations of 10 p.p.m. or less).

In figure 2 (*a*) we show the comparison of the theoretical $\chi(T)/\chi(0)$ with the Mössbauer results by Steiner and Hüfner [57], which yields $T_K=2$ K. The agreement of theory and experiment is good despite some scattering in the data at low T. The Mössbauer hyperfine field [57] as a function of field and temperature is displayed in figure 2 (*b*). Except for the saturation hyperfine field there are no further adjustable parameters. The best fit was obtained for $H^{sat}=84$ kG, but somewhat different values for H^{sat} are also acceptable.

Although the overall agreement is reasonable we note some discrepancy in the high-field low-temperature magnetization. This difference cannot be attributed to interactions between impurities (the experiments were performed with only a few p.p.m. of Fe), but may arise from reminiscent orbital contributions. If the orbital singlet is not completely formed, an orbital high-field magnetization of opposite sign to the spin magnetization is expected to develop [58].

3.5. *The Kondo system Cr*Cu

As for Fe*Ag* the Kondo temperature is small [59] and hence impurity–impurity interactions are relatively important, so that it is experimentally necessary to study the ultra-dilute limit to investigate single-impurity properties. On the other hand, one has to compromise with the observability of the effect, which is proportional to the impurity concentration. The interaction effects are expected to be most noticeable in the bulk susceptibility, which directly measures the local and intersite correlations. In summary, the Cr*Cu* system represents a much less favourable situation than Fe*Cu* for the observation of the single-site Kondo effect [12].

We determine T_K from the zero-field specific heat. The data of Triplett and Phillips [51] and Impens and Dupré [60] are shown in figure 3 (*a*). A comparison with the theory yields $T_K \sim 1{\cdot}5$ K. There is some dispersion between the two sets of data and so, the theoretical curves for $n=5$ and 3 have been displayed for comparison. There is good agreement of the Impens and Dupré results with the $n=5$ curve. While the maximum in the data of Triplett and Phillips is in better accordance with $n=3$, the high- and low-

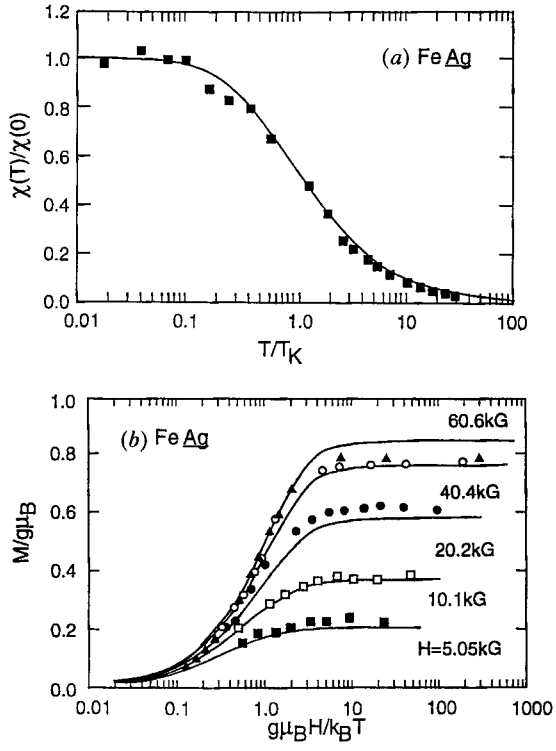

Figure 2. Comparison of theory for the $S=n/2$ multi-channel Kondo model with experimental data for dilute FeAg alloys [13]. (*a*) Zero-field susceptibility normalized to its $T=0$ value as a function of T for $T_K=2$ K (squares: Mössbauer data of Steiner *et al.* [57]). (*b*) Magnetization in units of $g\mu_B$ in constant field as a function of $(g\mu_B H/k_B T)$. The solid lines are the theoretical curves for $S=2$, $g=2$ and $T_K=2$ K. The field is in kG. The magnetization data has been scaled with a hyperfine saturation field of 84 kG [57].

temperature tails are clearly above the theoretical $n=3$ curve, so that the entropy associated with the data is closer to that of a $S=5/2$.

The specific heat measurements in the presence of a magnetic field by Triplett and Phillips [52] are shown in figure 3 (*b*). Using $n=5$, $T_K=1{\cdot}5$ K, and $g=2$ we get a reasonably good agreement with the experimental data. The $H=0$ curve is added for comparison. In large fields there is a small discrepancy in the position and height of the peak.

Measurements of the susceptibility as a function of T by Vochten *et al.* [61] are shown in figure 3 (*c*). Impurity–impurity interactions become important at lower temperatures. These interaction effects can in part be quenched by a moderate external magnetic field. The single site impurity theory predicts a decrease of the susceptibility with the field. Experimentally, however, an increase of χ for low fields (at low T) is observed. We attribute this reversed trend to the quenching of the RKKY interactions between the impurities by the field. It is then expected that the data in a small magnetic field is closer to the theoretical curve for zero field than the zero-field data. Shown in figure 3 (*c*) is also the calculated zero-field susceptibility. The agreement between theory and experiment for χ is reasonable for $T>3T_K$. The value of the zero-temperature susceptibility requires $n=2S=5$, in accordance with the specific heat results.

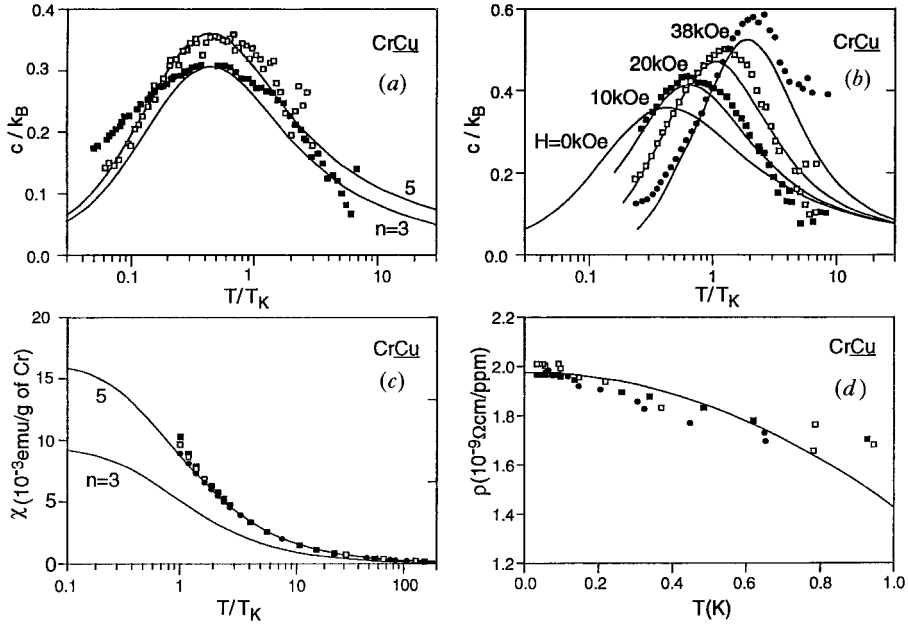

Figure 3. Comparison of theory for the $S=n/2$ multi-channel Kondo model with experimental data for dilute Cr*Cu* alloys [12]. (*a*) Impurity specific heat over the Boltzmann constant as a function of T/T_K for $T_K=1{\cdot}5$ K. The solid curves are the theoretical curves for $n=3$ and 5. The solid squares are the 51 p.p.m. data of figure 1 of Triplett and Phillips [51] and the open squares the 106 p.p.m. data of figure 1 of Impens and Dupré [60]. (*b*) Impurity specific heat over k_B in the presence of a magnetic field (0, 10, 20, 38 kOe) as a function of T/T_K. The data are taken from figure 2 of Triplett and Phillips [52] and correspond to a 51 p.p.m. sample. The solid curves are the theoretical results for $S=5/2$, $T_K=1{\cdot}5$ K, $g=2$ and the several fields. The zero-field curve is included for comparison but the data is omitted. (*c*) Impurity susceptibility in emu/g of Cr taken from figure 2 of Vochten *et al.* [61] as a function of T/T_K with $T_K=1{\cdot}5$ K. The data corresponds to a 12·7 p.p.m. sample. The solid squares correspond to 3·96 kOe, the open squares to 8·51 kOe and the dots to 12·64 kOe. The solid curve is the theoretical result for $S=5/2$, $g=2$ and zero-field. (*d*) Impurity contribution to the resistivity per p.p.m. Cr in zero magnetic field, taken from figure 1 of Daybell and Steyert [62] as a function of T. The solid squares are data for a 12 p.p.m. sample, the open squares for sample *a* of 28 p.p.m. and the dots for the sample *b* of 28 p.p.m. The solid curve is the theoretical curve for $S=5/2$ and $T_K=1{\cdot}5$ K.

The resistivity difference per p.p.m. of one alloy with 12 p.p.m. and two with 28 p.p.m. of Cr in Cu [62] are shown in figure 3 (*d*) together with the theoretical curve, (3.7), for $n=5$ and $T_K=1{\cdot}5$ K. The agreement is reasonable, confirming that the Fermi-liquid picture is valid. The shape of the theoretical curve is somewhat sensitive to the choice of T_K. For higher T the experimental curve departs from the T^2 behaviour, since the Kondo resistivity is expected to become logarithmic around T_K [63].

4. The undercompensated impurity spin case

In this section we briefly summarize the analytical and numerical results for the undercompensated spin situation, i.e., $S>n/2$. Here the impurity spin is only partially compensated, since there are not enough conduction electron channels to yield a singlet ground-state. This leaves an effective spin degeneracy in zero field at low temperatures

of $(2S+1-n)$. This situation could be related to the integer-valent limit of impurities with two magnetic configurations like Tm [18].

4.1. *Some analytic results*

Some of the low-T properties can be understood in terms of the zero-temperature magnetization, which is given by the following analytic expression [17, 25, 32]

$$M=\left(S-\frac{n}{2}\right)-\frac{in}{4\pi^{3/2}}\int_{-\infty}^{\infty}d\omega\frac{\exp\left[i\omega(2/\pi)\ln\left(H/T_H\right)\right]}{\omega-i0}\left(\frac{in\omega+0}{e\pi}\right)^{in\omega/\pi}$$
$$\times\exp\left[-(2S-n)|\omega|\right]\frac{\Gamma(1+i\omega/\pi)\Gamma(0{\cdot}5-i\omega/\pi)}{\Gamma(1+in\omega/\pi)}, \tag{4.1}$$

where T_H is given by

$$T_H=(2\pi/n)\left[(n/2e)^{n/2}/\Gamma(n/2)\right]T_K. \tag{4.2}$$

The small-field behaviour ($H\ll T_K$) is extracted by closing the contour through the lower half-plane and the leading contributions arise from the cut along the imaginary axis [17, 32]

$$M=\left(S-\frac{n}{2}\right)\left\{1+\frac{n/4}{\ln\left(H/T_K\right)}+\frac{(n/4)^2\ln\left|\ln\left(H/T_K\right)\right|}{\left[\ln\left(H/T_K\right)\right]^2}+\ldots\right\}. \tag{4.3}$$

Hence, even a small magnetic field aligns the remaining spin of magnitude $(S-\frac{1}{2}n)$ and this remaining spin is only weakly coupled to the electron gas (logarithmic singularities). The zero-field zero-temperature entropy of the impurity can be obtained from (2.25) and the asymptotic solution of the integral equations for $\lambda\to+\infty$ [26, 27, 29]

$$S(T=0,\ H=0)=\ln\left(|2S-n|+1\right). \tag{4.4}$$

In a small magnetic field the remaining spin is quenched and the $T=0$ entropy is zero, i.e., a singlet. At high temperatures, on the other hand, the impurity free energy is given by (3.6), i.e., the impurity behaves as a free spin in a magnetic field.

4.2. *Some numerical results*

We are going to limit ourselves to present a few illustrative examples, in particular for $n=1$. For more details the reader is referred to [29, 42].

The entropy is a measure of the effective degrees of freedom of the impurity at a given temperature and field. Figures 4(*a*) and 4(*b*) show the entropy as a function of T in constant field for $n=1$ and the half-integer spins $S=1/2$ and $3/2$, respectively. The entropy for $S=1/2$ agrees with the results by Rajan *et al.* [3] and is included for comparison, to emphasize that the cases $S=1/2$ and $S>1/2$ behave differently. All cases with $S>n/2$ are qualitatively similar. In zero field the entropy varies monotonically between $\ln(2S)$ (since $n=1$) at low T and $\ln(2S+1)$ for $T\gg T_K$. For $S=1/2$ the field shifts the crossover between the two asymptotical values towards higher temperatures, because the magnetic field suppresses the degrees of freedom of the impurity. If $S>1/2$ the degeneracy of the impurity at low T is lifted by the magnetic field and the entropy at $T=0$ ($H\neq0$) is zero. Hence, in addition to the Kondo crossover, in the undercompensated case there is a second crossover related to the Zeeman splitting, which occurs approximately at $T\sim H$.

The specific heat is given by the temperature derivative of the entropy in constant field. The specific heat as a function of Ts shown in figures 5(*a*) and 5(*b*) for the same set

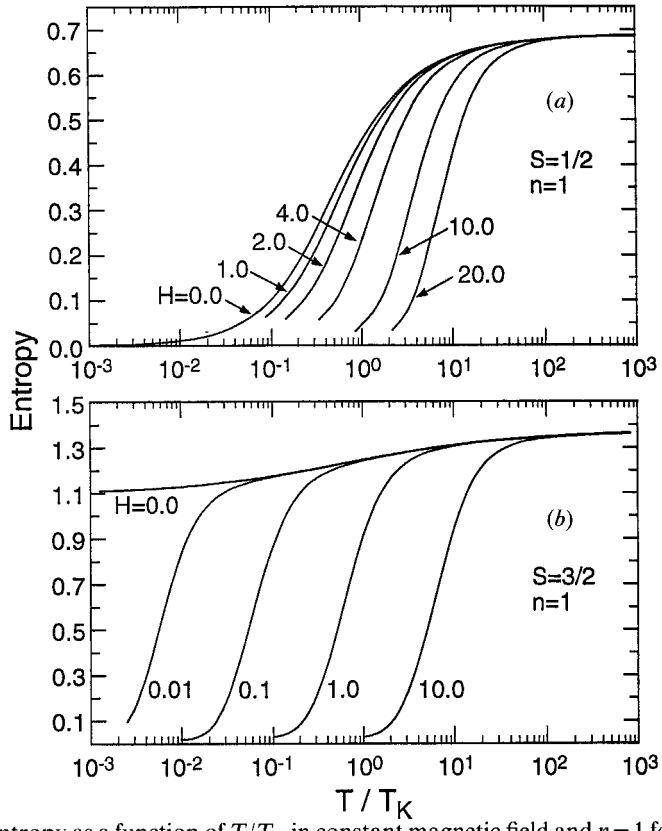

Figure 4. Entropy as a function of T/T_K in constant magnetic field and $n=1$ for (*a*) $S=1/2$ and (*b*) $S=3/2$. The field intensity H is given in units of T_K [42].

of spin and magnetic field values as in figure 4. For spin 1/2 ($n=1$) the specific heat has a peak which shifts towards higher temperatures as the field is increased (see also [3]). The height of the peak also grows with field and asymptotically (on a logarithmic scale characteristic of asymptotic freedom) approaches the value of a free-spin Schottky anomaly. For $S>1/2$ (undercompensated situation) again the zero field and $H\neq 0$ cases are qualitatively different, because the Zeeman splitting lifts the degeneracy of the ground-state. The height of the peak of the zero-field Kondo specific heat dramatically decreases with the spin [3, 42] and disappears in the classical spin limit, i.e., as $S\to\infty$ (note that the change in entropy from $T=0$ to ∞ is $\ln[(2S+1)/(2S)]$). The large resonance at about $T\sim H$ in figure 5 (*b*) refers to the Schottky anomaly due to the Zeeman splitting. Since $n=1$, for $H\ll T_K$ the Schottky peak is the one of a spin $S-1/2$, while if $H\gg T_K$ it corresponds to a spin S. A smooth crossover between these two regimes is obtained. Hence, if $H\ll T_K$ the specific heat in the undercompensated case has two independent peaks, one corresponding to the Zeeman splitting of the ground-multiplet and one to the Kondo screening.

The magnetization increases monotonically with the magnetic field and for a given field M increases as T is reduced. The saturation values of M as $T\to 0$ depend on the magnetic field, as a consequence of the Kondo effect. The magnetic field quenches the Kondo screening only partially, so that M does not reach the value S, but the saturation value is always larger than $S-n/2$. At high temperatures, i.e. $H\ll T$, on the other hand,

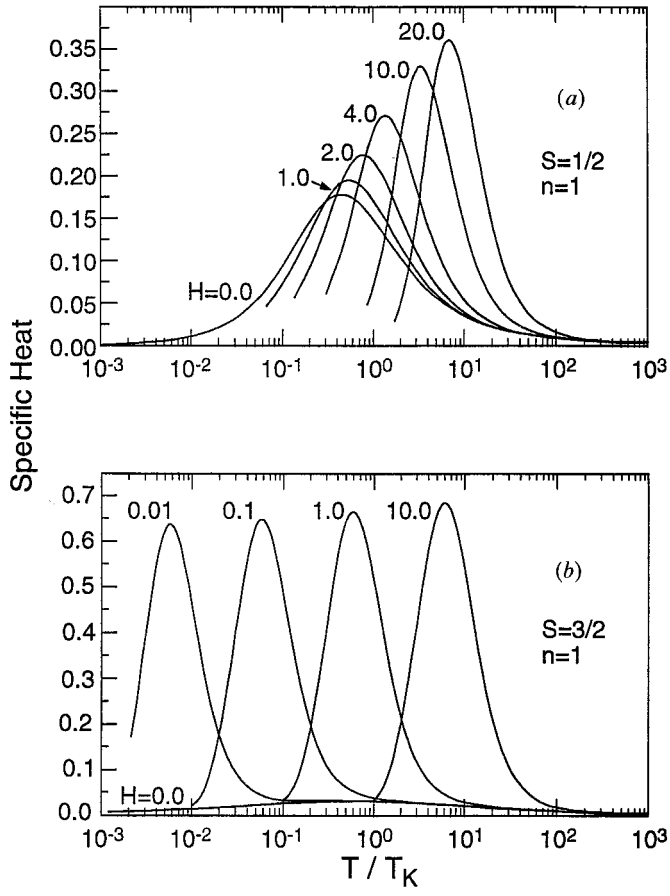

Figure 5. Specific heat as a function of T/T_K in constant magnetic field and $n=1$ for (*a*) $S=1/2$ and (*b*) $S=3/2$. The field intensity H is given in units of T_K[42].

$M \sim H/T$ and the susceptibility follows the expected Curie law (corresponding to a spin $S-n/2$ if $T \ll T_K$ and to a spin S if $T \gg T_K$).

Finally, we briefly discuss the magnetic susceptibility for $n=1$ as a function of T. Again $S=1/2$ behaves differently as a consequence of the singlet ground-state. For $S=1/2$ the susceptibility is maximum at low T if H is small, as a consequence of the Kondo resonance. For large fields, on the other hand, χ has its maximum at about $T \sim H$, reminiscent of the free-spin behaviour. At high temperatures χ follows a Curie law. For $S \neq 1/2$, i.e. the undercompensated spin case, χ is more conveniently presented on a double-log plot. χ for $S=3/2$ is shown in figure 6. The $H=0$ Curie law appears then as a straight line. There is, however, a smooth change in the Curie constant, since the effective spin is S at high T and $S-1/2$ at low T. The magnetic field lifts the degeneracy at low T and significantly reduces χ, which nevertheless remains finite due to the Kondo-spin-compensated degree of freedom. The maximum of χ at $T \sim H$ has the same origin as the Schottky anomaly of the specific heat.

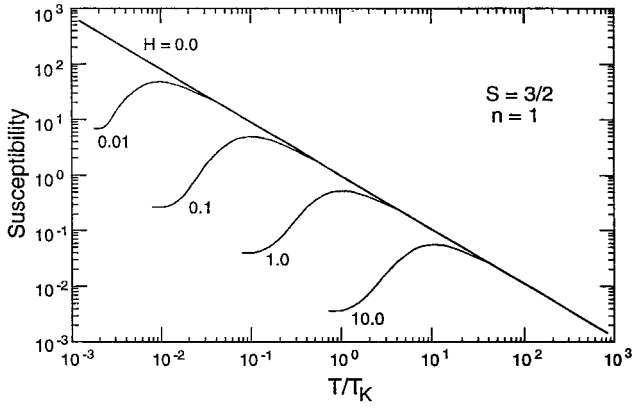

Figure 6. Susceptibility as a function of T/T_K in constant magnetic field and $n=1$ for $S=3/2$. The field intensity H is given in units of T_K [42].

5. The overcompensated impurity spin case

In this section we discuss the physical properties of the overcompensated Kondo effect $n>2S$. In this case there are more conduction electron channels than necessary to compensate the impurity spin. The remaining conduction electron spin $n-2S$ is delocalized and gives rise to critical behaviour. We first present some analytical and numerical results and then discuss two applications: the quadrupolar Kondo effect and the electron assisted tunnelling of an atom in a double-well potential close to the strong coupling fixed point. Both applications refer to an effective impurity spin $S=1/2$, so that most of our discussion will be focused on this case.

5.1. *Some analytic results*

As for the undercompensated case some of the low-T properties can be understood in terms of the zero-temperature magnetization, which is given by the following analytic expression [17, 25, 32]

$$M=-\frac{in}{4\pi^{3/2}}\int_{-\infty}^{\infty}d\omega\frac{\exp\left[i\omega(2/\pi)\ln\left(H/T_H\right)\right]}{\omega-i0}\left(\frac{in\omega+0}{e\pi}\right)^{in\omega/\pi}$$
$$+\frac{\sinh\left(2S\omega\right)}{\sinh\left(n\omega\right)}\frac{\Gamma(1+i\omega/\pi)\ \Gamma(0{\cdot}5-i\omega/\pi)}{\Gamma(1+in\omega/\pi)}, \tag{5.1}$$

where T_H is given by (4.2). The small-field behaviour ($H\ll T_K$) is extracted by closing the contour through the lower half-plane and the leading contribution arises from the pole due to $\sinh(n\omega)$ closest to the real axis (but $\omega\neq 0$). The susceptibility diverges with a power law given by [25, 28]

$$\chi=H^{(-1+2/n)},\qquad n>2,\qquad S<n/2. \tag{5.2}$$

This result has also been obtained using conformal field theory [64]. The exponent vanishes if $n=2$ and $S=1/2$ and a logarithmic dependence on the field [25, 27, 28, 65] is obtained as a consequence of a double pole at $\omega=-i\pi/2$. Note that the critical exponent in (5.2) only depends on the number of channels, but not on the spin.

An interesting quantity is the zero-field zero-temperature entropy of the impurity, which again can be obtained from (2.25) and the asymptotic solution of the integral equations for $\lambda\to+\infty$ [26, 27, 29]

$$S(T=0,\ H=0)=\ln\left\{\sin\left[\pi(2S+1)/(n+2)\right]/\sin\left[\pi/(n+2)\right]\right\}. \tag{5.3}$$

Hence for $S<n/2$ the ground-state entropy corresponds to a fractional spin. It can be shown that in the presence of a magnetic field the ground-state is a singlet, i.e., the entropy is zero. The entropy has then an essential singularity for $H=T=0$. At high temperatures, on the other hand, the impurity behaves like a free spin in a magnetic field.

The low-T (zero-field) susceptibility, $\chi(T)$, and the specific heat over T, C/T, diverge for an overcompensated spin with critical behaviour given by [24, 26–28]

$$\chi \sim (T/T_K)^{\tau-1}, \qquad C/T \sim (T/T_K)^{\tau-1}, \tag{5.4}$$

where $\tau=4/(n+2)$. This result has also been obtained via conformal field theory [64]. Comparing with (5.2) we note that the scaling dimensions of the temperature and the field are different. Hence, the limits $T\to 0$ and $H\to 0$ cannot be interchanged. For $n=2$ and $S=1/2$ (two-channel Kondo model) the critical exponents vanish and again a logarithmic dependence on the temperature arises [26–28, 65].

The instability of the fixed point to a magnetic field has been confirmed both by numerical renormalization group calculations [66] and by conformal field theory [67]. Furthermore, it has been established that the fixed point is also unstable to a channel-symmetry-breaking field [66, 67], but it is stable against an exchange anisotropy if $S=1/2$ or $S=(n-1)/2$ [66, 67]. These relevant fields produce a crossover to a Fermi-liquid fixed point. Other treatments of the model include the bosonization of the conduction electrons [68] and a $1/n$ expansion [69].

5.2. *Some numerical results*

Properties at intermediate temperatures and the simultaneous effects of temperature and field can only be obtained numerically. For simplicity, we restrict ourselves to $S=1/2$; results for larger spins can be found in the literature [29].

The numerical zero-field results for the specific heat over T and the susceptibility as a function of T/T_K are shown in figures 7 (*a*) and 7 (*b*), respectively, for $n=1,\ldots,6$ [28]. The case $n=1$ corresponds to the standard Kondo problem and is included for comparison. For $n=1$ the ground-state is a singlet and both χ and C/T are finite as $T\to 0$ (Fermi-liquid behaviour). As discussed above for $n=2$ a logarithmic and for $n>2$ a power-law dependence is obtained at low T. Note that within our numerical accuracy all the susceptibility curves cross each other at about $T=0{\cdot}1T_K$. According to (5.3) for $n>2S$ the $T=0$ entropy is non-zero and the effective spin fractional. This is consistent with the divergence in the susceptibility, equation (5.4).

In a finite field the situation is qualitatively different. If $H\neq 0$ the susceptibility is always finite (for all n and S) and consequently the ground-state is expected to be a singlet. Hence, the zero-temperature entropy is zero irrespective of the strength of the field, $S(T=0, H\neq 0)=0$ [26, 28, 65, 70], and has an essential singularity at the critical point $T=H=0$. As a consequence of the singlet ground-state for $H\neq 0$ the impurity has Fermi-liquid properties over a limited range of temperature. For small fields the characteristic Fermi-liquid energy scale is not T_K, but a function of the field-strength and depends on the scaling dimensions for the field and temperature [28, 29, 70], $d_H=2/n$ and $d_T=4/(n+2)$. These low-T (Fermi-liquid) properties have to be calculated using the second numerical method discussed in section 2.5.

The entropy curves in constant fields as a function of T/T_K for $S=1/2$ and $n=2$ are shown in figure 8 (*a*) (see [28]). The results for other values of $n>2$ are similar and can be found in [28, 29]. In zero-field the entropy of the impurity interpolates smoothly between the value $\frac{1}{2}\ln(2)$ given by equation (5.3) for low temperatures and the

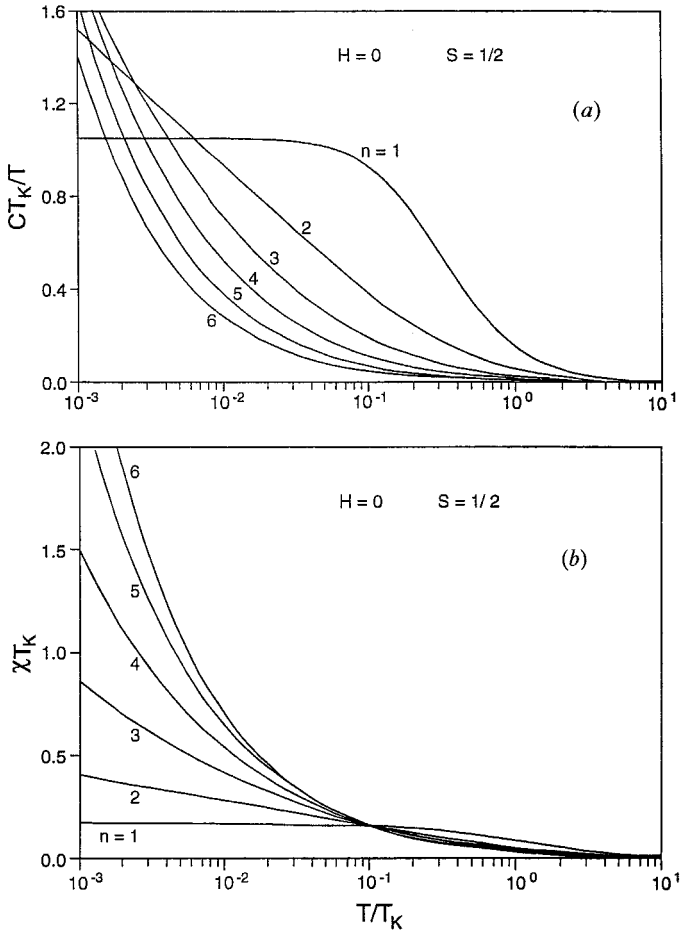

Figure 7. Numerical zero-field results for a spin-1/2 impurity [28]: (*a*) the specific heat over temperature and (*b*) the susceptibility as a function of T/T_K for $n=1,\ldots,6$. Note that both C/T and χ diverge as $T\to 0$ if $n>1$.

asymptotic free spin entropy, ln(2), at high T. In a non-vanishing field, the entropy tends to zero proportionally to T at low temperatures as discussed above. At high T, i.e. for $T \gg H$, again the asymptotic free spin value of ln(2) is reached. The drop in the entropy at low T, consequence of the magnetic field, begins on a temperature scale of the order H^2/T_K for $n=2$, i.e., at very low T if the field is small. The reduction of the entropy (when T is reduced) at high temperatures is a consequence of the Kondo screening. Hence, there are two independent energy scales involved, namely H^2/T_K and T_K, which are well separated if the field is small, as seen in figure 8 (*a*). The situation is similar for larger n. As n increases the Kondo screening is less pronounced. The field-dependent energy scale can be shown to be $T_K(H/T_K)^{1+2/n}$ using the scaling dimensions d_T and d_H of the temperature and the field, respectively. For very large n this energy scale is just the magnetic field. This is consistent with the gradual decrease of the Kondo compensation with n, so that for $n\to\infty$ the impurity behaves like a free spin with Zeeman splitting. These results for $n>1$ are qualitatively different from the traditional Kondo problem ($n=1$), where there is only one energy scale, namely T_K.

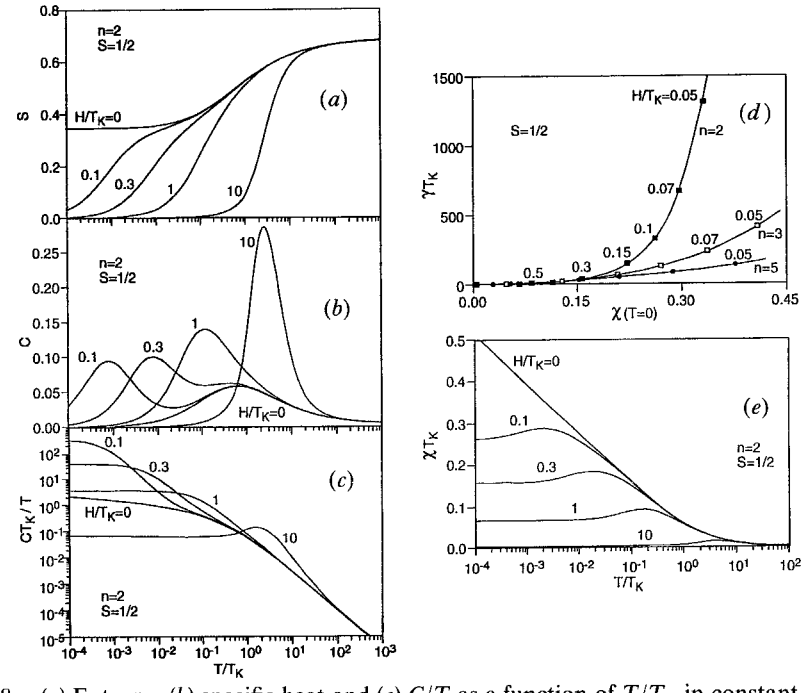

Figure 8. (*a*) Entropy, (*b*) specific heat and (*c*) C/T as a function of T/T_K in constant field for $S=1/2$ and $n=2$ [28] and five values of the field $H/T_K=0, 0{\cdot}1, 0{\cdot}3, 1$ and 10. The entropy is singular at $H=T=0$: if $H=0$ the entropy at $T=0$ is finite and equal to $\frac{1}{2}\ln(2)$, while it vanishes if $H\neq 0$. For $H\neq 0$ the low T entropy and specific heat are proportional to T. The $H=0$ specific heat curve shows the Kondo resonance. A two-peak structure in C is observed in small fields, which at high fields merge into a Schottky anomaly. Giant γ values are obtained in small fields. The shoulders in C/T are due to the incipient Schottky anomaly in higher fields. (*d*) γ values as a function of the zero-temperature susceptibility for $n=2$, 3 and 5 with the field as the parameter [28]. Note the rapid increase of γ as $H\to 0$. (*e*) Susceptibility as a function of T/T_K in constant field for $S=1/2$ and $n=2$ [28] and five values of the field $H/T_K=0, 0{\cdot}1, 0{\cdot}3, 1$ and 10. The logarithmically divergent response in zero-field is clearly seen. The shoulders correlate with the field-dependent peak in the specific heat.

The specific heat as a function of T/T_K in constant field for $n=2$ and $S=1/2$ is shown in figure 8 (*b*). These curves just correspond to the slope of those in figure 8 (*a*). The zero-field specific heat has one peak at $T\sim T_K$, which arises from the Kondo screening that reduces the entropy from ln (2) to the zero temperature value $\frac{1}{2}$ln (2) given by equation (5.3). In a small magnetic field, e.g. $H=0{\cdot}1T_K$, this Kondo peak basically remains unchanged but at low T a second peak develops, consequence of the second energy scale. The two peaks are well separated at low fields and merge into one at intermediate fields, e.g. $H\sim T_K$. At very high fields the free-spin Schottky resonance is asymptotically reached on a logarithmic scale (characteristic of asymptotic freedom). For larger values of n the results [28] are qualitatively similar, but the height of the resonance for low fields is large, since a large amount of entropy has to be removed. As $n\to\infty$ the height of the peak (only one can be seen) is that of a spin 1/2 Schottky anomaly. Again the results for $n>1$ are qualitatively different from the traditional Kondo problem ($n=1$), where there is only one energy scale, namely T_K.

For $H \neq 0$ the low-temperature specific heat is proportional to T and can be characterized by a coefficient γ. In figure 8 (*c*) we show C/T in constant field as a function of T/T_K for $n=2$ and $S=1/2$. The $H=0$ curve does of course not saturate as $T \to 0$, but γ is finite if H is non-zero. A similar behaviour is obtained for larger values of n [28]. For $n>1$, C/T increases dramatically at low T if the field is small, giving rise to giant γ values. A maximum in C/T arises for larger fields, i.e., C/T does no longer decrease monotonically with T, which is the consequence of the developing Schottky anomaly. At very high temperatures ($T \gg H$) the curves approach the high-temperature Kondo asymptotics.

In figure 8 (*d*) the γ-value (as obtained by extrapolating C/T to zero-temperature) [28, 29] is plotted against the $T=0$ susceptibility for $n=2, 3$ and 5. γ/χ, which is the inverse of the Wilson ratio, grows rapidly as $H \to 0$. For instance, for $n=2$ and $H=0{\cdot}1T_K$ the ratio is about 1260, i.e., 200 times larger than for the traditional Kondo problem. This is in first place due to the giant γ values, required to quench the large zero-temperature zero-field entropy. The low-field γ/χ ratios decrease with the number of orbitals. Since one gradually approaches a Schottky anomaly with increasing n, the fraction of entropy removed via a linear specific heat (Fermi liquid) has necessarily to decrease. For large H, γ/χ asymptotically reaches the value $2\pi^2/3n$. A more detailed analysis [70] of the increase of γ as $H \to 0$ shows that γ is approximately inversely proportional to the field energy scale $T_K(H/T_K)^{1+2/n}$, i.e., $\gamma \propto H^{-2}$ for $n=2$.

We had obtained similar results for $n=2$ in [65]. The γ values obtained there are substantially smaller than those reported here, as a consequence of the extrapolated non-vanishing $T=0$ entropy for $H \neq 0$. The giant γ values are actually the cause of the imprecision in the procedure employed in [65].

Affleck and Ludwig [64] calculated using conformal field theory that for $H=0$ in the overcompensated case

$$\left(\frac{\chi_{imp}}{\chi}\right)\Big/\left(\frac{C_{imp}}{C}\right)=\frac{1}{18}\left(2+\frac{2}{n}\right)(2+n)^2.$$

For $n=2$, $S=1/2$ this yields 8/3.

The susceptibility as a function of T for constant field [28] and $n=2$ is shown in figure 8 (*e*). For $H=0$ the susceptibility shows the critical behaviour already discussed above (logarithmic in T for $n=2$). χ decreases monotonically with field, but has a maximum as a function of T. This maximum in $\chi(T)$ correlates with the low T peak of the specific heat.

5.3. *The quadrupolar Kondo effect*

The quadrupolar Kondo effect was introduced by Cox [19] as a possible mechanism to quench the orbital and spin degrees of freedom of the uranium 5f shell in the heavy-fermion compound UBe_{13}. Kondoesque quadrupolar mechanisms have been proposed previously by Fulde and Loewenhaupt [71] in the context of rare earth ions with crystalline field splittings interacting with conduction electrons. UBe_{13} is a superconductor [72] for temperatures below 0·9 K and has very unusual thermal and magnetic properties in both, the superconducting and the normal, phases. The low-T specific heat in the normal phase is very large and only weakly field-dependent [73]. The resistivity shows a maximum as a function of T, similar to other heavy-fermion compounds [73]. The coherent scattering of the lattice at low T is superimposed with the superconductivity below T_c. For $T>2$ K the resistivity decreases with T, typical of incoherent scattering off Kondoesque impurities, and the magnetoresistivity is large

and negative. The magnetic susceptibility is roughly Curie–Weiss-like, but surprisingly almost field-independent [74]. The inelastic neutron scattering data [75] are consistent with a broad Lorentzian-shaped quasi-elastic peak in the dynamic susceptibility of width ~ 15 meV.

In order to explain the lack of field-dependence of the electronic specific heat and the susceptibility, as well as the broad structure observed by neutron scattering, Cox [19, 76] proposed the quadrupolar Kondo effect (which, however, does not account for the strong negative magnetoresistivity). The main assumptions of the model are the following. (i) The stable f-shell configuration of the U ions is $5f^2$ and according to Hund's rules this leads to a ground-multiplet with total angular momentum $J=4$ (isoelectronic to Pr^{3+} ions). (ii) The cubic crystalline field splits the $J=4$ multiplet into a Γ_1-singlet, a Γ_3-doublet and Γ_4 and Γ_5-triplets. The Γ_3 non-Kramers doublet is assumed to the the one with lowest energy. (iii) The excited Γ_4-triplet is also relevant, since it explains a Schottky anomaly in the specific heat and the coupling to the Γ_3 via the magnetic field yields a van Vleck susceptibility (nearly field-independent) and could as well account for the broad structure in $\chi''(\omega)/\omega$. The specific heat is then almost field-independent [19, 76, 77].

The Kondo effect is incorporated [19] by hybridizing the 5f electrons with the conduction states and by considering virtual excitations into the $5f^1$ configuration (the rare-earth analogue is Ce^{3+}) with a $J=5/2$ Hund's rule ground-multiplet, which is split into a Γ_7-doublet and a Γ_8-quartet in cubic symmetry. Typically the Γ_7 has lower energy. The conduction electrons hybridizing with f electrons must be in the partial-wave states $j=5/2$ and $j=7/2$. A nonvanishing matrix element between the Γ_3-states of $5f^2$ and the Γ_7-states of the $5f^1$ configuration can be obtained via the $j=5/2$ partial wave, in particular with the conduction states having Γ_8-symmetry. By means of a canonical transformation of the Schrieffer–Wolff-type (projecting the $5f^1$ states out), one obtains the following exchange interaction [19],

$$H_{ex}=\tfrac{1}{2}J\mathbf{S}\cdot[\boldsymbol{\sigma}_8(0)+\boldsymbol{\sigma}'_8(0)], \tag{5.5}$$

where $J>0$, $\mathbf{S}$ are the pseudospin operators for $S=1/2$ representing the Γ_3-doublet and $\boldsymbol{\sigma}$ is the vector of Pauli matrices. $\boldsymbol{\sigma}_8$ and $\boldsymbol{\sigma}'_8$ denote two pseudospins 1/2 representing the four Γ_8 states at the U-ion site. Hamiltonian (5.5) is of the general form of the spin-1/2 two-channel Kondo model.

Although some of the approximations leading to the quadrupolar Kondo Hamiltonian remain to be proven (e.g. the choice of the configurations and the crystalline field splitting scheme), the model itself is exciting in view of its marginal critical behaviour. Below we discuss the implications of the exact solution of the overcompensated Kondo problem on the physical properties of these heavy-fermion U-systems. Note that the 'magnetic field' in the Kondo Hamiltonian corresponds to the tetragonal (quadrupolar) splitting related to a deformation of the cubic symmetry. The 'magnetization' is the quadrupolar moment and the 'magnetic susceptibility' represents actually the quadrupolar susceptibility [19, 77, 78].

The $T=0$ susceptibility diverges logarithmically as $H\to 0$. Consequently in cubic symmetry the impurity system is unstable with respect to a local tetragonal lattice deformation [65, 77, 78]. In the case of a compound this instability leads to either a structural transition or to long-range quadrupolar order. The elastic energy associated with a local lattice deformation is of the form $\frac{1}{2}aH^2$, where a is proportional to the elastic constant c_{11} (H is the quadrupolar splitting which is proportional to the tetragonal deformation). The free energy of the system is then the one of the impurity

and the elastic energy, $F(H,T)+\frac{1}{2}aH^2$. The equilibrium position for the lattice deformation is $\langle S_z\rangle = aH$. At $T=0$ there is always a non-trivial solution, i.e. with $H\neq 0$, which is the energetically favourable solution. This equilibrium value of H is gradually reduced with increasing temperature and vanishes above a critical temperature, which is given by $\chi(T=T_c,\ H=0)=a$. In view of the logarithmic dependence of the susceptibility with T, however, T_c may be exponentially small. Neither a structural phase transition nor quadrupolar long-range ordering has been observed in UBe_{13}, but it cannot be excluded that T_c is below the experimental range [78].

As T is lowered C/T increases logarithmically until T_c is reached and eventually saturates with a giant γ-value as $T\to 0$. The fingerprint of the quadrupolar Kondo effect in the specific heat as a function of T is the two maxima [65] discussed in subsection 5.2, in addition to a peak corresponding to the second order transition at T_c. The quadrupolar moment decreases monotonically with T and vanishes above T_c in cubic symmetry.

Associated with the critical behaviour is a divergent correlation length. Hence, even if the concentration of U-ions is very small, they are going to interfere with each other at low T. This interference competes with the local lattice distortion induced by a single quadrupolar Kondo ion. The two-impurity two-channel Kondo problem has recently been studied by means of Wilson's numerical renormalization group technique [79]. The renormalization group flows yield a rich phase diagram as a function of single-site and inter-impurity couplings. Several stable, unstable and marginal fixed points were found.

It has been suggested that the quadrupolar Kondo effect has been observed in the alloy $U_xY_{1-x}Pd_3$ [80, 81]. For $x=0{\cdot}2$ the resistivity and the specific heat show a $\ln(T)$ behaviour. The extrapolated change in the entropy between very high and low T is approximately $(R/2)\ln(2)$. The magnetoresistivity is small and negative. Other experimental results are in disagreement with the predictions of the $S=1/2$ two-channel Kondo model. At very low T the resistivity data can be fitted by

$$R(T)/R(0)=1-(T/T_K)^k, \qquad k=1{\cdot}13\pm 0{\cdot}04,$$

while theoretically $k=1/2$ [82]. This recent result [82] is in disagreement with earlier work [83, 84]. Also the experimental scaling dimension of the field is larger than the theoretical one for the single impurity. The double peak structure in the specific heat is absent. Controversial is also the fact that the specific heat is more sensitive to a magnetic field than the resistivity [81]. Hence, the field appears to have a different influence on the transport properties than on the thermodynamics. Other possible quadrupolar Kondo effect systems are $U_xTh_{1-x}Ru_2Si_2$, $x\leqslant 0{\cdot}07$ [85] and $Ce_{0{\cdot}1}La_{0{\cdot}9}Cu_{2{\cdot}2}Si_2$ [86], which also display non-Fermi-liquid properties at low T.

5.4. *Electron assisted tunnelling of an atom in a double-well potential*

Since the pioneering work of Caldeira and Leggett [87] the subject of tunnelling particles coupled to a heat bath has attracted great interest [88–90], in particular also in the context of metallic glasses. In a metallic glass an atom may tunnel between two possible positions possessing levels close in energy, which can be represented as a two-level system (TLS). The tunnelling atom is placed in a double-well potential and can then spontaneously hop from one position to the other. These tunnelling transitions are rare and a much more efficient mechanism is the electron assisted tunnelling, in which the scattering of a conduction electron off the tunnelling atom induces the transition. The multiple scattering of electrons with the TLS creates electron–hole excitations of

arbitrarily small energy in the electron gas [20, 21, 91, 92], giving rise to logarithmic singularities in the scattering matrix and other physical quantities, in close analogy to the Kondo [63] and X-ray threshold [93] problems. Problems involving logarithmic singularities in all physical properties to all orders in the perturbation expansion are suitable candidates for renormalization group (RG) treatments. In the RG procedure high energy states with energies close to the band-edge are gradually eliminated from the system giving rise to renormalizations of the coupling parameters, vertices and self-energies. The successive reduction of the band cut-off energy (ultraviolet cut-off) eventually leads to a fixed point, which determines the critical properties of the model. For so-called non-commutative models the relevant fixed point is usually related to a strong coupling situation and isomorphic to the n-channel Kondo problem [28].

There is experimental evidence for the strong coupling between the TLS and the conduction electrons. In metallic glasses the tunnelling gives rise to an additional contribution to the low-T specific heat which is linear in T. The specific heat contribution linear in T in high temperature superconductors has also been attributed to TLS-tunnelling. An anomalously large acoustic saturation intensity as well as a $\ln(T)$ dependence was observed in the acoustic absorption of the metallic glass PdSiCu [94, 95]. The strong coupling of the TLS to electrons appears to be responsible for anomalies in the ultrasonic absorption and dispersion in amorphous superconductors [96, 97]. The specific heat of superconducting Nb is also strongly affected by the tunnelling of H, D and O impurities [98]. Some physical properties of A15 compounds have as well been attributed to the strong interaction of TLS with electrons [99].

A general form of the Hamiltonian of a TLS interacting with a degenerate Fermi gas [20] consists of three terms, $H = H_0 + H_{\rm TLS} + H_{\rm int}$. Here H_0 is the kinetic energy of the conduction electrons,

$$H_0 = \sum_{k,\alpha,s} \epsilon_k a^\dagger_{k\alpha s} a_{k\alpha s}, \tag{5.6a}$$

where $a^\dagger_{k\alpha s}$ creates a conduction electron with momentum $k = |\mathbf{k}|$, spin s and partial wave of orbital angular momentum l and its z-projection m labelled by the index α. The states of the TLS are parametrized in terms of Pauli matrices

$$H_{\rm TLS} = -\tfrac{1}{2}\Delta_0 \boldsymbol{\sigma}^z + \tfrac{1}{2}\Delta_1 \boldsymbol{\sigma}^x, \tag{5.6b}$$

where Δ_0 is the energy splitting between the two states of the double-well and Δ_1 is the intrinsic tunnelling rate. The interaction of the conduction electrons with the TLS can be written as

$$H_{\rm int} = \sum_{k,k',\alpha,\beta,s,i} a^\dagger_{k\alpha s} V^i_{\alpha\beta} a_{k'\beta s} \boldsymbol{\sigma}^i, \tag{5.6c}$$

where $i = x, y, z$. The k-dependence of the potentials $V^i_{\alpha\beta}$ can be neglected (it is irrelevant, since the infrared singularities are determined by states close to the Fermi energy), although the important angular dependence (i.e., α, β) has to be kept [92]. The V^z-terms represent the difference of the scattering amplitudes for the two positions of a rigid TLS, while the V^x and V^y-terms describe the electron-assisted tunnelling, i.e., electron scattering with simultaneous tunnelling of the atom. These terms arise from the fluctuations of the potential barrier due to fluctuations in the electron density. The spin of the electron is not altered in the scattering process. Note that $|V^x|, |V^y| \ll |V^z|$, since atoms are much heavier than electrons [92]. $H_{\rm TLS}$ can be diagonalized by means of a rotation of the $\boldsymbol{\sigma}$ matrices to give an effective splitting $E = (\Delta_0^2 + \Delta_1^2)^{1/2}$ and hence, we may choose $\Delta_1 = 0$ without loss of generality.

The renormalization of the Hamiltonian (5.6) is simplest within the poor man's scaling approach, in which conduction states with energies close to the band cut-off are successively eliminated reducing in this way the effective band cut-off D' gradually. As a consequence the coupling parameters in the Hamiltonian are renormalized, obeying the following differential equations [92]

$$\partial V^s_{\alpha\beta}(x)/\partial x = -2i\rho \sum_{i,j} \epsilon^{ijs} \sum_{\gamma} V^i_{\alpha\gamma}(x) V^j_{\gamma\beta}(x), \tag{5.7}$$

where $x = \ln(D/D') > 0$ and ρ is the density of states. The logarithmic dependence on the cut-off is due to the electron–hole excitations with arbitrarily small energy, while the ϵ^{ijs} Levi-Civita symbols enter as a consequence of the Pauli matrices describing the TLS and the $V^i_{\alpha\beta}$ being non-commutative. Note that the general form of the Hamiltonian remains invariant under the renormalization procedure, except for the change in the coupling amplitudes. The initial conditions for the differential equations (5.7) are that the $V^i_{\alpha\beta}(x=0)$, i.e. for $D'=D$, are equal to the bare coupling parameters. Equation (5.7) refers to the renormalization of the model in leading logarithmic order. Renormalization to higher order does not affect the general structure of the differential equations and with minor modifications the argumentation below remains valid.

Let us first consider the special case when

$$V^i_{\alpha\beta} V^j_{\beta\gamma} - V^j_{\alpha\beta} V^i_{\beta\gamma} \tag{5.8}$$

is zero for all i and j. This case is known as the *commutative model* [100]. The right-hand-side of (5.7) vanishes for all s, α and β, so that all the coupling constants remain unrenormalized and do not scale into a strong coupling regime, resembling in this way the X-ray threshold problem [93]. The tunnelling rate decreases with temperature and at low T the dynamics is frozen into one of the two potential minima. The fermion excitation spectrum can be 'bosonized', showing a close analogy with a TLS coupled to a phonon bath. The commutative model is realized, e.g., if only one partial wave plays a role in the scattering off the TLS.

The *non-commutative model* corresponds to the case when (5.8) is non-zero for at least one pair of matrices [92]. The physical fixed point of the non-commutative model is in general a strong coupling one, i.e., the invariant coupling parameters of the model grow when D' is lowered. As a consequence due to the electron assisted hops the atom cannot be localized in one of the two potential minima [101]. This situation is mathematically analogous to the Kondo problem where the impurity is spin-compensated by the conduction electrons, quenching in this way the magnetic properties at low temperatures. The analogy is of course only a formal mathematical one. The TLS itself corresponds to the Kondo impurity spin 1/2, the energy separation Δ of the two positions in the TLS has its analogy in the Zeeman splitting of the Kondo impurity spin, and the partial waves (orbital degrees of freedom) of the conduction electrons interacting with the TLS represent spin degrees of freedom of the conduction electrons in the Kondo problem. The spin of the conduction electrons interacting with the TLS corresponds to the channel index in the Kondo problem.

With the repeated application of the RG procedure the system eventually reaches a fixed point. Near the fixed point the vector space on which the matrices operate can be divided into invariant subspaces [92] whose scaling equations can be separately studied. We assume that one subspace μ is dominant and determines the properties of

the system. Close to the fixed point it is expected that the matrix character of $[V^i_{\alpha\beta}(x)]_\mu$ does not change with further scaling and can be factorized [92]

$$[V^i_{\alpha\beta}(x)]_\mu = [V^{*i}_{\alpha\beta}(\mu)]_\mu v^i_\mu(x), \tag{5.9 a}$$

where $v^i_\mu(x)$ is the amplitude that is still renormalized and the $[V^{*i}_{\alpha\beta}(\mu)]_\mu$ are the infinitesimal generators of an irreducible unitary representation of the rotation group satisfying the following equations

$$\mathrm{i}V^{*s}_{\alpha\beta}(\mu) = \sum_{i,j} \epsilon^{ijs} \sum_\gamma V^{*i}_{\alpha\gamma}(\mu) V^{*j}_{\gamma\beta}(\mu). \tag{5.9 b}$$

The different subspaces μ correspond to the different dimensionalities of the generators, i.e., to the different values of an effective 'spin' S_μ (with dimension $g_\mu = 2S_\mu + 1$).

Assuming that only one subspace μ is relevant at low temperatures and small energies (i.e., this subspace decouples from the rest of the states), the effective Hamiltonian is of the form

$$H_{\mathrm{int}} = V\boldsymbol{\sigma} \cdot \sum_{\alpha,\beta,s,k,k'} A^\dagger_{k\alpha s} \mathbf{S}_{\alpha\beta} A_{k'\beta s}, \tag{5.10}$$

where $A^\dagger$ and A are fermion operators for conduction states having the symmetry corresponding to the subspace μ. For spinless fermions and if the subspace is two-dimensional the problem reduces to the single channel Kondo problem [92]. If the spin of the electrons is not neglected the two-dimensional case corresponds to the two-channel Kondo model [21].

In general, if the subspace μ has dimension g the problem for spinless fermions is equivalent to the n-channel Kondo model with $n = g - 1$. In order to show this we consider the alternative exchange model (2.3) in which electrons of spin $n/2$ interact with an impurity of spin S_i. S_i in our case is a spin 1/2 represented by the vector of Pauli matrices $\boldsymbol{\sigma}$ in (5.10). The polynomial P defined by (2.4) is then of first order.

$$P[\boldsymbol{\sigma} \cdot \mathbf{s}_e] = a + b(\boldsymbol{\sigma} \cdot \mathbf{s}_e), \tag{5.11}$$

where a and b are constants. Since potential scattering is not relevant in the strong-coupling regime, the Hamiltonian (5.11) is the equivalent to (5.10) if spinless $A_{k\alpha}$ are considered. Although we do not provide rigorous results for the spin-degenerate case, we believe that the two spin-channels in (5.10) add together yielding an effective orbital subspace of dimension $g = 4S_\mu + 1$. This result is rigorous if the orbital subspace μ is two dimensional.

In summary, in a realistic situation at low T the atom is either localized in one of the potential minima (commutative model, e.g., when only one orbital partial wave is relevant) or not localized showing critical behaviour (non-commutative model, including spin-degeneracy). The latter corresponds to the overcompensated Kondo problem. Since spinless electrons are only of academic interest the completely spin-compensated Kondo case is not applicable. Below we discuss the consequences of the critical behaviour on the TLS.

The susceptibility is the response of the TLS to an asymmetry of the energy levels of the two positions of the double-well potential, $\Delta (= H)$. Since the susceptibility diverges as H and T tend to zero the symmetric TLS is unstable [28]. Assume we have initially a symmetric TLS and allow a small coupling to a phonon deformation field. The divergent susceptibility of the TLS and the coupling to the phonons will induce a local distortion in the neighbourhood which then leads to a level splitting. At high T this

splitting is zero and there is a critical temperature T_c below which $\Delta \neq 0$ is the stable situation. The transition at T_c is continuous, i.e. Δ tends to zero as $T \to T_c$, in complete analogy to the quadrupolar Kondo effect discussed in section 5.3.

We have assumed that only one subspace μ is relevant, which is believed to be the case at low T. The validity of our arguments is then restricted by the role of other subspaces. When the T is raised or for higher energy excitations, other representations will influence the physical properties.

Since the ground-state equilibrium situation for an isolated TLS corresponds to $\Delta \neq 0$, the ground-state entropy vanishes and a Fermi-liquid-like picture applies [28], i.e., the susceptibility is finite and the specific heat is proportional to T. The γ values can become very large, giving rise to giant γ/χ ratios. For a small asymmetry the specific heat shows a double peak structure which is specially evident for $n=2$. At larger asymmetries ($\Delta \sim T_K$) the peaks merge into one.

There has been recent experimental evidence that a TLS may be responsible for the resistivity of a metallic constriction [102]. The differential resistance of metal point contacts containing structural disorder shows the characteristic logarithmic behaviour and a power law dependence at low T

$$R(T)/R(0) = 1 - aT^{1/2}.$$

This result may be explained by the $n=2$, $S=1/2$ Kondo model. The effect of magnetic impurities has been ruled out, so that this observation may be the first direct application of the overcompensated Kondo model to metallic glasses. Annealing gave further support to this conjecture [102], since the structural deformation caused by the TLS may be washed away by annealing. Other possible realizations of multichannel Kondo behaviour are the Kondo-like effect of the motion of Ge on the resistivity of $Pb_{1-x}Ge_xTe$ [103] and the logarithmic T-dependence of the low-T resistivity in heavily doped conducting polymers [104].

6. Heisenberg chain with impurity

Since Bethe's diagonalization of the isotropic spin-1/2 Heisenberg chain [105], several integrable generalizations were discovered, for instance, (*a*) the anisotropic chain [106], (*b*) the SU(2)-invariant chain or arbitrary spin S [22,23,33,34], (*c*) systems of arbitrary number of components and SU(N) symmetry [38,107], and (*d*) the Heisenberg chain of spin S with an impurity of arbitrary spin S' [24,108,109] (some of these systems are reviewed in [110]). Here we briefly review case (*d*) which for antiferromagnetic coupling has low-T properties closely related to the multichannel Kondo problem [24]. Again three situations have to be distinguished. (i) If $S'=S$ the impurity just corresponds to one more site in the chain and consequently its properties are identical to those of the 'bulk'. (ii) If $S'>S$ the spins neighbouring the impurity are not able to compensate the impurity spin S' into a singlet at low T (undercompensated spin). (iii) If $S'<S$ again a perfect compensation of the impurity spin by the neighbouring lattice sites cannot take place and the remaining spin degrees of freedom induce critical behaviour (overcompensated spin).

6.1. *Model and its diagonalization*

We consider an SU(2)-invariant Heisenberg chain of N sites with arbitrary spin S (Babujian–Takhtajan model [22,23]) and periodic boundary conditions, i.e., a ring of length N so that $S_{N+1} \equiv S_1$. The impurity is assumed to be located on the mth link, i.e. between the mth and $(m+1)$th sites, and interacts only with both neighbouring sites.

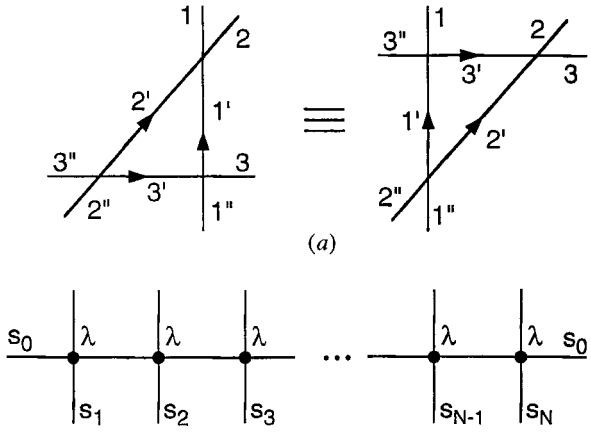

Figure 9. (*a*) Schematic representation of the triangular relation [37], equation (6.1). On the right-hand-side first particles 1 and 2 scatter, then 1 and 3 and finally 2 and 3. On the left-hand-side first 2 and 3 scatter, then 1 and 3 and finally 1 and 2. The final result of both processes is the same. (*b*) Schematic diagram of the monodromy matrix [33, 34].

The interaction must be of a special type [24, 108, 109] to preserve the integrability of the model. The starting point is a set of commuting transfer matrices, whose local vertex weights ${}_{SS'}R(\lambda)$ satisfy the triangular Yang–Baxter relations [37],

$$R^{12}(\lambda)R^{13}(\lambda+\mu)R^{23}(\mu)=R^{23}(\mu)R^{13}(\lambda+\mu)R^{12}(\lambda), \tag{6.1}$$

which guarantees the integrability of the system by construction. In figure 9(*a*) we show a schematic representation of the two processes defined by (6.1) which yield identical results.

We introduce the monodromy matrix $\hat{I}_S(\lambda)$ [24, 33, 34]

$$\hat{I}_S(\lambda)={}_{SS}R^{01}(\lambda)\,{}_{SS}R^{02}(\lambda)\ldots{}_{SS}R^{0m}(\lambda)\,{}_{SS'}R^{0\mathrm{imp}}(\lambda)\,{}_{SS}R^{0m+1}(\lambda)\ldots{}_{SS}R^{0N}(\lambda), \tag{6.2}$$

where the matrix product is carried out in the auxiliary space labelled with index '0' of dimension $(2S+1)$. Note that the vertex weight for the impurity (spin S') has been inserted between the sites m and $(m+1)$. A schematic representation of the monodromy matrix [24, 33, 34] is shown in figure 9(*b*). The auxiliary space is denoted by the horizontal line, all others by vertical lines. Taking the trace over the incoming and outgoing auxiliary lines (i.e. by forming a ring) we obtain the transfer matrix $\mathbf{T}_S(\lambda)$

$$\mathbf{T}_S(\lambda)=\mathrm{Tr}_0\,[\hat{I}_S(\lambda)]. \tag{6.3}$$

As a consequence of the triangular Yang–Baxter relation [37] satisfied by all the vertex weights, the transfer matrices for different values of the parameter λ commute,

$$[\mathbf{T}_S(\lambda),\mathbf{T}_S(\mu)]=0. \tag{6.4}$$

Hence, there exists a basis of states that diagonalizes $\mathbf{T}_S(\lambda)$ for all λ simultaneously. The Hamiltonian, i.e. the energy associated with the transfer matrix, is then constructed according to

$$H=\frac{\mathrm{d}}{\mathrm{d}\lambda}\ln \mathbf{T}_S(\lambda)\Big|_{\lambda=0}. \tag{6.5}$$

In the absence of an impurity this procedure leads to the Babujian–Takhtajan SU(2)-invariant Heisenberg chain of spin S. A special case of the Babujian–Takhtajan model is the standard Heisenberg model of spin 1/2.

The ferromagnetic state, i.e. the state with all spins aligned, is an obvious eigenstate of the transfer matrix. Other states can be constructed by flipping spins. With each spin-flip we associate one spin-rapidity (representing the momentum and energy of the excitation), so that for M spin-flips the state is represented by a set of M rapidities $\{\Lambda_l\}$. In order to become an eigenstate of $\mathbf{T}_S(\lambda)$ for all λ the Λ_l have to satisfy the following discrete Bethe ansatz equations [24]

$$\left(\frac{\Lambda_n+\mathrm{i}S}{\Lambda_n-\mathrm{i}S}\right)^N \frac{\Lambda_n+\mathrm{i}S'}{\Lambda_n-\mathrm{i}S'} = -\prod_{l=1}^{M} \frac{\Lambda_n-\Lambda_l+\mathrm{i}}{\Lambda_n+\Lambda_l-\mathrm{i}}, \tag{6.6}$$

where $n=1,\ldots,M$. The second factor on the left-hand-side of (6.6) is due to the impurity. The energy of the antiferromagnetic chain is given by [34]

$$E=-\sum_{l=1}^{M} \frac{S}{\Lambda_l^2+S^2}, \tag{6.7}$$

and the magnetization by $NS+S'-M$. The Hamiltonian is just the sum over the interactions between neighbouring sites. The interaction between two arbitrary neighbouring lattice sites of spin S is given by the Babujian–Takhtajan model. The interaction between the spins $\mathbf{S}_m$, $\mathbf{S}_{m+1}$ and $\mathbf{S}'$ is more complicated and can be expressed as a linear combination of products of irreducible tensor operators.

6.2. *Thermodynamic Bethe ansatz equations*

Equations (6.6) are very similar to the set (2.18), which are the Bethe ansatz equations for the alternative model to the multichannel Kondo problem, defined by (2.3). This model involved a gas of electrons of spin $s_e=n/2$ and an impurity of spin S (equations (2.18) actually refer to $S=n/2$, but the results are straightforwardly generalized to arbitrary impurity spin). In analogy to (2.19) the solutions of (6.6) are given by strings of length n

$$\Lambda_j^{n,\alpha}=\Lambda_j^n+\mathrm{i}(n+1-2\alpha)/2, \qquad \alpha=1,\ldots,n, \tag{6.8}$$

where Λ_j^n is the centre of the string and a real number. The procedure to derive the thermodynamic Bethe ansatz equations is now very similar to that in section 2.4 (see equation (2.23)) and the equations only differ by the driving term, which for the Heisenberg chain becomes (note that $\lambda=2\Lambda$) [24, 34]

$$-\frac{2\pi}{T}\delta_{l,2S}[2\cosh(\pi\Lambda)]^{-1}. \tag{6.9}$$

Hence, the limit $|\Lambda|\to\infty$ corresponds to the strong-coupling low-temperature fixed point, and the small Λ regime is most important at high T. The thermodynamic Bethe-ansatz equations for this model were recently solved numerically by one of us [111]. The low-T solution is very analogous to the one of the multichannel Kondo problem,

and hence we expect similar properties for the impurity in the Heisenberg chain. The free energy for the lattice ('host' chain) and the impurity are given by [24]

$$F_{\text{host}} = F^0_{\text{host}} - NT \int d\Lambda\, [2\cosh(\pi\Lambda)]^{-1} \ln[1+\eta_{2S}(\Lambda)],$$

$$F_{\text{imp}} = F^0_{\text{imp}} - T \int d\Lambda\, [2\cosh(\pi\Lambda)]^{-1} \ln[1+\eta_{2S'}(\Lambda)], \tag{6.10}$$

where F^0_{host} and F^0_{imp} are constants given by

$$F^0_{\text{host}} = \frac{N}{2}[\psi(\tfrac{1}{2}) - \psi(\tfrac{1}{2}+S)],$$

$$F^0_{\text{imp}} = \tfrac{1}{2}\{\psi(\tfrac{1}{2}+\tfrac{1}{2}|S-S'|) - \psi[\tfrac{1}{2}+\tfrac{1}{2}(S+S')]\}, \tag{6.11}$$

with ψ being the digamma function.

6.3. *Properties of the impurity*

Comparing the impurity and host parts in equations (6.10) and (6.11) it is evident that if $S' = S$ the impurity just corresponds to adding one more link to the host chain. We now briefly summarize the low-temperature results for the three situations: $S' = S$, $S' > S$ and $S' < S$. At high T, i.e. $T \gg 1$ the impurity behaves like a free spin S' in a magnetic field.

(i) In the absence of a magnetic field the ground-state consists of strings of length $2S$ which are densely distributed (no holes). The ground-state energy is given by

$$E = -\frac{1}{2}\int d\omega\, \hat{\rho}_{2S}(\omega) \exp(-S|\omega|) \frac{\sinh(S\omega)}{\sinh(\omega/2)}, \tag{6.12}$$

where $\hat{\rho}_{2S}(\omega)$ is the Fourier transform of the distribution function of the real rapidities corresponding to strings of length $2S$ [24]

$$\hat{\rho}_{2S}(\omega) = [2\cosh(\omega)/2]^{-1}\left\{1 + \frac{1}{N}\exp\{[S - \max(S,S')]|\omega|\}\frac{\sinh[\min(S,S')\omega]}{\sinh(S\omega)}\right\}. \tag{6.13}$$

The first term represents the lattice and the second one the impurity contribution. Inserting (6.13) into (6.12) we obtain after integrating, $E = F^0_{\text{host}} + N^{-1}F^0_{\text{imp}}$, as expected from equations (6.10) and (6.11).

(ii) If the field H is non-zero the ground-state distribution $\rho_{2S}(\Lambda)$ has holes and satisfies an integral equation of the Fredholm type. If the magnetic field is sufficiently small this integral equation can be reduced to a sequence of Wiener–Hopf equations and can be solved by iteration [24, 34]. For $S' = S$ the impurity is just one more site in the chain so that $F_{\text{imp}} = F_{\text{host}}/N$ and

$$F^S_{\text{imp}}(T=0,H) = \tfrac{1}{2}[\psi(\tfrac{1}{2}) - \psi(\tfrac{1}{2}+S)] - \frac{SH^2}{2\pi^2}\left[1 + \frac{S}{|\ln H|} - \frac{S^2(\ln|\ln H|)}{(\ln H)^2} + \ldots\right], \tag{6.14a}$$

in agreement with Babujian's result [34]. (6.14 *a*) shows the existence of logarithmic singularities in the small-field susceptibility of the chain. For $S' > S$, on the other hand, we obtain for small fields [24]

$$F^{S'}_{\text{imp}}(T=0,H)=\tfrac{1}{2}\{\psi[\tfrac{1}{2}+\tfrac{1}{2}(S'-S)]-\psi[\tfrac{1}{2}+\tfrac{1}{2}(S'+S)]\} \\ -(S'-S)H\left[1+\frac{S}{|\ln H|}-\frac{S^2(\ln|\ln H|)}{(\ln H)^2}+\ldots\right]; \qquad (6.14\,b)$$

hence, at $T=0$ the impurity has an effective spin $(S'-S)$ that is weakly coupled to the spins of the chain as manifested by the logarithmic corrections. Finally, if $S' < S$ the impurity is overcompensated [24]

$$F^{S'}_{\text{imp}}(T=0,H)=\tfrac{1}{2}\{\psi[\tfrac{1}{2}+\tfrac{1}{2}(S-S')]-\psi[\tfrac{1}{2}+\tfrac{1}{2}(S+S')]\}-AH^{1+1/S}, \qquad (6.14\,c)$$

where

$$A=\left(\frac{e}{\pi}\right)^{1/2}\frac{\sin(\pi S'/S)\,\Gamma[1+1/(2S)]\,\Gamma(1+S)]^{1/S}}{\cos(\pi/2S)\,\Gamma[\tfrac{1}{2}+1/(2S)]\;\pi^{2/S}(1+S)}.$$

As a consequence of the field-dependent term in (6.14 *c*) the susceptibility diverges as $H^{-1+1/S}$ as $H\to 0$. Hence, the collective behaviour of the impurity interacting with the magnetic chain leads to critical properties. If $S=1$ (and $S'=1/2$), the field-dependent term in (6.14 *c*) is not regular in H but logarithmic, $-(2/\pi^3)H^2|\ln H|$. Hence, the susceptibility in this case diverges logarithmically as $H\to 0$ (as for the quadrupolar Kondo effect).

(iii) For the zero-temperature entropy we again have to distinguish several cases. If $S'=S$, i.e. for the Babujian–Takhtajan model, the entropy of the ground-state vanishes independently of the field,

$$S(H, T=0)=0. \qquad (6.15\,a)$$

Hence, the ground-state is a singlet. For $S' > S$ we obtain [24]

$$S(H=0, T=0)=\ln[2(S'-S)+1], \\ S(H\neq 0, T=0)=0, \qquad (6.15\,b)$$

i.e., in zero field the undercompensated impurity case leads to an effective spin $(S'-S)$ as discussed above. If the field is non-zero the Zeeman splitting lifts the spin-degeneracy and a singlet is obtained. Finally, if $S' < S$ we have [24]

$$\left.\begin{aligned} &S(H=0, T=0)=\ln\{\sin[\pi(2S'+1)/(2S+2)]/\sin[\pi/(2S+2)]\}, \\ &S(H\neq 0, T=0)=0, \end{aligned}\right\} \qquad (6.15\,c)$$

so that the effective zero-field degeneracy is not an integer, but fractional. This again is consistent with the critical behaviour discussed above. These results are in close analogy to the overcompensated multichannel Kondo problem.

(iv) We now discuss the low-T specific heat and susceptibility of the impurity. For $S'=S$ the ground-state is always a singlet and the system behaves like a marginal Fermi-liquid. The specific heat is proportional to T at low temperatures [112]. If $S' > S$ the remaining spin degeneracy of $(S'-S)$ gives rise to a Schottky anomaly for $H\sim T$ and the zero-field susceptibility diverges with a Curie-law corresponding to an effective spin $(S'-S)$.

For the overcompensated case $S' < S$ $C/T$and χ diverge with a power law (unless $S=1$ and $S'=1/2$) in zero-field as $T \to 0$ [24]

$$C/T \sim T^{-1+4/(2S+2)}, \qquad \chi \sim T^{-1+4/(2S+2)}. \tag{6.16a}$$

If $S=1$ and hence $S'=1/2$, on the other hand, the critical exponent vanishes and the divergence is logarithmic [24]

$$C/T \sim \ln(\pi/T), \qquad \chi \sim \ln(\pi/T). \tag{6.16b}$$

Since the field and the temperature have different scaling dimensions, $1/S$ and $4/(2S+2)$, respectively, the limits $T \to 0$ and $H \to 0$ cannot be interchanged. Note that the critical exponents only depend on the spin of the host but not on S' (as long as $S' < S$). At slightly larger values of H and T again two peaks are obtained [111] in the specific heat, as well as a maximum in χ as a function of T if $H \neq 0$, in complete analogy to the overcompensated n-channel Kondo problem.

In summary, we briefly discussed the construction of an integrable model consisting of an impurity of spin S' embedded into a Babujian–Takhtajan Heisenberg chain of spin S, its exact diagonalization and properties for antiferromagnetic coupling [24]. The properties of the impurity are very analogous to those of the multichannel Kondo problem ($n=2S$) of arbitrary impurity spin S'. It should be mentioned that for the Heisenberg chain with ferromagnetic coupling the impurity, independently of its spin, is locked into the critical behaviour of the lattice, i.e., at low temperatures the specific heat is proportional to $T^{1/2}$ (ferromagnetic magnons) and the susceptibility diverges as T^{-2} with logarithmic corrections [113].

The singular behaviour discussed above appears (at a first glance) to be inconsistent with recent renormalization group studies of impurities in spin-1/2 chains [114]. From the renormalization group flow diagram it is concluded that the only stable critical points correspond to a completely unperturbed chain or else a chain with a break at the impurity site (i.e., the periodic or open chain, respectively). In the open chain case, but not in the periodic, a remnant impurity spin may also be present. However, for antiferromagnetic coupling of the impurity to the chain the open chain has no leftover impurity in the low-energy spectrum. A more detailed study of the system around the integrable point in parameter space, lead to the conclusion that the integrable impurity model corresponds to a non-generic multi-critical point [115].

On the other hand, these properties of integrable models are not restricted to isolated impurities, but are valid for concentrated systems as well. Consider for instance the standard Heisenberg chain of spin 1/2 with a concentration x of impurity spins S. In zero-field the ground-state [116] is a singlet for finite x, but non-Fermi-liquid-like for $x \to 0$. It is concluded that as a function of x the single impurity fixed-point is non-generic, in agreement with the results in [115]. The Heisenberg chain of alternating spins 1/2 and spins S ($x=1/2$) has been investigated previously [117]. For further generalizations to translational invariant lattice models with second-next-nearest neighbour interactions see [118].

7. Concluding remarks

We have reviewed the n-channel Kondo model for an impurity of spin S, where n and S are independent model parameters. The first thorough analysis of this model was by Nozières and Blandin [15] within the framework of a renormalization group treatment to next to leading logarithmic order. They found that in leading logarithmic

order the different channels are decoupled, but they become strongly coupled in higher than leading order. This picture was confirmed by numerical renormalization group calculations [66, 116] and the Bethe-ansatz solution of the model [16, 17, 25]. The Bethe-ansatz results show that the spins of n conduction electrons are glued together to form an effective spin $s_c = n/2$, which then couples to the impurity spin. Three situations have to be distinguished: (i) the undercompensated impurity, (ii) the totally compensated spin and (iii) the overcompensated impurity spin. The physical properties are qualitatively different for the three cases. The analytical and numerical solution of the thermodynamic Bethe-ansatz equations provide deep insight into the physical properties of the systems that can be described by the model.

Only the $n = 2S$ case exhibits Fermi-liquid behaviour, i.e., the ground-state of the system is a singlet for all values of the magnetic field. The low-T properties are determined by the Kondo peak which is on resonance with the Fermi level in view of the electron–hole symmetry of the n-channel Kondo model. The specific heat as a function of T has a peak at about $0{\cdot}5T_K$ which is to be associated with the thermal population of the Kondo resonance or equivalently with the lifting of the Kondo spin-compensation. At low T the specific heat is proportional to T, with a γ value inversely proportional to T_K, while at high T logarithmic corrections appear, indicative of the asymptotic freedom. The $T = 0$ susceptibility is finite and approaches the expected Curie-law at high T. We have compared the exact Bethe-ansatz results with the experimental data for three 3d-electron impurity systems [11–13], namely Fe*Cu*, Fe*Ag* and Cr*Cu*. The agreement is remarkably good, in particular for Fe*Cu*, which is probably the best studied 3d-impurity system.

In section 4 we reviewed the case of an undercompensated Kondo impurity, $S > n/2$. Since there are not enough channels to yield a singlet ground-state, the impurity is only partially compensated by the conduction electrons at low T, leaving an effective spin-degeneracy (in zero-field) of $(2S + 1 - n)$. An arbitrary small magnetic field lifts the degeneracy of the ground-state, leaving a singlet. At finite T this gives rise to a Schottky anomaly in the specific heat and a peak in the susceptibility at $T \sim H$. Hence, if $H \ll T_K$ the specific heat shows a two-peak structure, one peak associated with the Zeeman splitting of the ground-multiplet and the other one with a broad Kondo resonance. For intermediate or large fields (compared with T_K) they merge into one peak. The susceptibility follows a Curie law, the Curie constant corresponds to a spin S at high T and to an effective spin $S - n/2$ at low T. Logarithmic corrections reflect the asymptotic freedom at low and high T. The integer-valent limit of impurities with two magnetic configurations like Tm could be related to this situation [18].

If $n > 2S$ the number of conduction-electron channels is larger than required to compensate the impurity spin. This is the most exciting case, since the strong-coupling fixed point is not the usual $J \to \infty$ fixed point, but one with finite coupling strength [120]. This unusual fixed point has properties reminiscent of critical behaviour. The entropy is essentially singular as H and T tend both to zero. The susceptibility diverges with a power of the field and temperature. Fingerprints of the overcompensated system are the two-peak structure in the specific heat at low fields and extremely large γ-values as $H \to 0$. Two possible applications of this situation (for $S = 1/2$) are the quadrupolar Kondo effect ($n = 2$) [19, 80] and the low-T fixed point of a two-level system interacting with conduction electrons (an atom in a double-well potential with electron-assisted tunnelling) [20, 21, 102]. In the former case the magnetic field corresponds to a quadrupolar splitting, while in the latter one it represents the asymmetry of the double well. In both cases the coupling to the phonons has to be included. Due to the divergent

quadrupolar susceptibility a tetragonal distortion is induced by the quadrupolar Kondo impurity in cubic symmetry below a critical temperature T_c. For the same reason the symmetric double-well configuration is not stable for a tunnelling atom at very low T.

Mechanisms similar to the multichannel Kondo effect have been proposed in the context of high temperature superconductivity [121] to generate the marginal Fermi-liquid properties observed in the cuprates. There are also some common features between the two-impurity (single-channel) Kondo problem [122] and the multichannel Kondo problem. (i) For strong ferromagnetic Ruderman–Kittel–Kasuya–Yosida (RKKY) coupling the two impurity spins lock into a triplet which is then spin-compensated by the conduction electrons much like in the $S=1$ two-channel Kondo problem [123]. (ii) For electron–hole symmetry the regions of attraction of the two stable fixed-points are separated by an unstable fixed-point with marginal Fermi liquid properties [124], similar to those of the overcompensated n-channel Kondo problem. There are as well aspects in common, i.e. non-Fermi-liquid-like properties, between the overcompensated n-channel Kondo problem and a model of a local orbital coupled through repulsive interactions to both the hybridizing and screening channels of a conduction band [125–127]. The n-channel Kondo problem is also closely related to Wess–Zumino field-theories.

The same properties as for the n-channel Kondo impurity hold for a magnetic impurity of spin S' embedded in the antiferromagnetic Babujian–Takhtajan Heisenberg chain of spin S [24]. Again, if $S'>S$ the impurity is undercompensated, if $S'=S$ the impurity is just one more link in the chain and if $S'<S$ the overcompensated situation is realized. At low T and for small H the Bethe-ansatz equations are identical to those of the Kondo problem.

Finally, we would like to point out that there exists an integrable one-dimensional two-band model of interacting electrons with a Bethe ansatz solution that has formally the same structure as model (2.2) for $n=2$ [128]. The model involves a crystalline field splitting between the two bands and an exchange potential between electrons. The model, a sketch of its solution and some properties are presented in the Appendix.

Acknowledgment

The support of the Department of Energy under grant DE-FG05-91ER45443 is acknowledged.

Appendix: Two-band model with attractive and repulsive interactions

In this Appendix we consider an integrable one-dimensional two-band model with attractive and repulsive interactions recently solved by one of us [128]. The interest in two-band models arises from the possibility that both, $3d_{x^2-y^2}$ and $3d_{z^2}$, orbitals may play a role in high T_c cuprates. The model consists of two parabolic bands of electrons of equal mass separated by a crystalline field splitting Δ. The Hamiltonian is the following

$$H=\sum_{m,\sigma}\int dx\, c^{\dagger}_{m\sigma}(x)(-\partial^2/\partial x^2)c_{m\sigma}(x)+\Delta\sum_{m,\sigma} m\int dx\, c^{\dagger}_{m\sigma}(x)c_{m\sigma}(x)$$

$$+c\sum_{m,m',\sigma,\sigma'}\int dx_1\int dx_2\,\delta(x_1-x_2)c^{\dagger}_{m\sigma}(x_1)c^{\dagger}_{m'\sigma'}(x_2)c_{m'\sigma}(x_2)c_{m\sigma'}(x_1), \qquad (A\,1)$$

where $m=1,2$ labels the electron bands and c is the strength of the δ-function *exchange* interaction. The interaction is attractive if the electrons form a spin-singlet (and orbital

triplet), while it is repulsive if the pair of electrons is in a spin-triplet (and orbital singlet). The two-electron scattering matrix has then formally the same structure as the one of model (2.2), i.e. it is of the form (2.6) and (2.7) if V^2 is replaced by c. Consequently also the discrete Bethe ansatz equations for Hamiltonian (A 1) are of the form of (2.8) for $n=2$, except for the impurity term ϕ_j in the equation for the charge rapidities which has to be dropped. The energy, however, is now given by $E=\Sigma_{j=1}^{N} k_j^2$, since the bands are parabolic. The classification of states and the thermodynamic Bethe ansatz equations [128, 129] for model (A 1) now follow along the same lines as described in section 2.

The low-temperature properties of model (A 1) are the following. The attractive interaction leads to the formation of Cooper-pair-type singlet bound-states [128, 129] and at $T=0$ there is no response to fields smaller than a threshold field H_c. A field larger than H_c is needed to overcome the binding energy of the Cooper pairs. The depaired electrons for $H>H_c$ occupy an unpaired-electron band and give rise to magnetization. If the field is only slightly larger than H_c, the magnetization is proportional to $(H-H_c)^{1/2}$ and the susceptibility diverges according to $(H-H_c)^{-1/2}$ (consequence of the one-dimensional van Hove singularity). The Cooper pairs are hard-core bosons, i.e., they have a Fermi surface and do not undergo condensation. Consequently there is no long-range order and the Cooper-pair bound-states do not cease to exist at finite T ($T_c=0$); in fact they are still the dominant states at low T. The Fermi surface of the Cooper pairs gives rise to a specific heat proportional to T at low temperatures, unless the Fermi level is at a van Hove singularity of one of the bands (then $T^{1/2}$ is the leading temperature dependence). The spectrum of elemental excitations [126] consists of four branches: (i) Cooper pair or charge excitations, (ii) spin excitations and (iii) two branches of interband excitations. Their dispersion is approximately parabolic and in zero magnetic field there are in general two Fermi surfaces. The momentum range of the interband transitions is coupled to the Fermi surface of the charge excitations.

References

[1] For a review see: SCHLOTTMANN, P., 1989, *Phys. Rep.*, **181,** 1.
[2] SCHLOTTMANN, P., 1984, *Z. Phys.* B, **57,** 23.
[3] RAJAN, V. T., LOWENSTEIN, J. H., and ANDREI, N., 1982, *Phys. Rev. Lett.*, **49,** 497.
[4] SCHLOTTMANN, P., 1987, *J. Magn. magn. Matter.* **63&64,** 205.
[5] HEWSON, A. C., and RASUL, J. W., 1983, *J. Phys.* C, **16,** 6799.
[6] SCHLOTTMANN, 1985, *J. appl. Phys.*, **57,** 3155.
[7] RASUL, J. W., and SCHLOTTMANN, P., 1989, *Phys. Rev.* B, **39,** 3065.
[8] BESNUS, M. J., HAEN, P., HAMDAOUI, A., HERR, A., and MEYER, A., 1990, *Physica* B, **163,** 571; ROSSEL, C., YANG, K. N., MAPLE, M. B., FISK, Z., ZIRNGIEBL, E., and THOMPSON, J. D., 1987, *Phys. Rev.* B, **35,** 1914.
[9] SCHLOTTMANN, P., 1993, *J. appl. Phys.*, **73,** 5412.
[10] LIN, C. L., WALLASH, A., CROW, J. E., MIHALISIN, T., and SCHLOTTMANN, P., 1987, *Phys. Rev. Lett.*, **58,** 1232.
[11] SACRAMENTO, P. D., and SCHLOTTMANN, P., 1990, *Solid-St. Commun.*, **73,** 747.
[12] SACRAMENTO, P. D., and SCHLOTTMANN. P., 1990, *Phys. Rev.* B, **42,** 743.
[13] SACRAMENTO, P. D., and SCHLOTTMANN, P., 1991, *Physica* B, **171,** 122.
[14] MÜHLSCHLEGEL, B., 1968, *Z. Phys.*, **208,** 94.
[15] NOZIÈRES, P., and BLANDIN, A., 1980, *J. Phys., Paris,* **41,** 193.
[16] ANDREI, N., and DESTRI, C., 1984, *Phys. Rev. Lett.*, **52,** 364.
[17] TSVELICK, A. M., and WIEGMANN, P., 1984, *Z. Phys.* B, **54,** 201.
[18] MAZZAFERRO, J., BALSEIRO, C. A., and ALASCIO, B., 1981, *Phys. Rev. Lett.*, **47,** 274; SCHLOTTMANN, P., 1982, *Valence Instabilities*, edited by P. Wachter and H. Boppart (North-Holland, Amsterdam), p. 471.
[19] COX, D. L., 1987, *Phys. Rev. Lett.*, **59,** 1240.
[20] ZAWADOWSKI, A., 1980, *Phys. Rev. Lett.*, **45,** 211.

[21] Muramatsu, A., and Guinea, F., 1986, *Phys. Rev. Lett.*, **57,** 2337.
[22] Takhtajan, L. A., 1982, *Phys. Lett.* A, **87,** 479.
[23] Babujian, H. M., 1982, *Phys. Lett.* A, **90,** 479.
[24] Schlottmann, P., 1991, *J. Phys. Condensed Matter*, **3,** 6617.
[25] Wiegmann, P. B., and Tsvelick, A. M., 1983, *Pis'ma Zh. Eksp. Teor. Fiz.*, **38,** 489; 1983, *JETP Lett.*, **38,** 591.
[26] Tsvelick, A. M., 1985, *J. Phys.* C, **18,** 159.
[27] Desgranges, H. U., 1985, *J. Phys.* C, **18,** 5481.
[28] Sacramento, P. D., and Schlottmann, P., 1991, *Phys. Rev.* B, **43,** 13294.
[29] Sacramento, P. D., and Schlottmann, P., 1991, *J. Phys. Condensed Matter*, **3,** 9687.
[30] Furuya, K., and Lowenstein, J. H., 1982, *Phys. Rev.* B, **25,** 5935.
[31] Rudin, S., 1983, *Phys. Rev.* B, **28,** 4825.
[32] Tsvelick, A. M., and Wiegmann, P. B., 1985, *J. statist. Phys.*, **38,** 125.
[33] Kulish, P. P., Reshetekhin, N., Yu, and Sklyanin, E. K., 1981, *Lett. Math. Phys.*, **5,** 393. 393.
[34] Babujian, H. M., 1983, *Nucl. Phys.* B, **215[FS7],** 317.
[35] Wiegmann, P. B., 1980, *Phys. Lett.* A, **80,** 163.
[36] Schlottmann, P., 1982, *Z. Phys.* B, **49,** 109; 1983, *Phys. Rev. Lett.*, **50,** 1967.
[37] Yang, C. N., 1967, *Phys. Rev. Lett.*, **19,** 1312; Baxter, R. J., 1972, *Ann. Phys. (N Y)*, **70,** 323.
[38] Sutherland, B., 1968, *Phys. Rev. Lett.*, **20,** 98.
[39] Schlottmann, P., 1983, *Z. Phys.* B, **51,** 49.
[40] Andrei, N., and Lowenstein, J. H., 1981, *Phys. Rev. Lett.*, **46,** 356; Filyov, V. M., Tsvelick, A. M., and Wiegmann, P. B., 1981, *Phys. Lett.* A, **81,** 175.
[41] Lee, K., and Schlottmann, P., 1987, *Phys. Rev.* B, **36,** 466.
[42] Sacramento, P. D., and Schlottmann, P., 1989, *Phys. Rev.* B, **40,** 431.
[43] Sacramento, P. D., 1991, Ph.D. thesis, Temple University, unpublished.
[44] Okada, I., and Yosida, K., 1973, *Prog. theor. Phys.*, **49,** 1483.
[45] Yoshimori, A., 1976, *Prog. theor. Phys.*, **55,** 67.
[46] Mihály, L., and Zawadowski, A., 1978, *J. Phys. Lett.* (Paris), **39,** L483.
[47] Wilson, K. G., 1975, *Rev. mod. Phys.*, **47,** 773.
[48] Rajan, V. T., 1983, *Phys. Rev. Lett.*, **51,** 308.
[49] Tholence, J. L., and Tournier, R., 1970, *Phys. Rev. Lett.*, **25,** 867.
[50] Steiner, P., Zdrojewski, W. v., Gumprecht, D., and Hüfner, S., 1973, *Phys. Rev. Lett.*, **31,** 355; Steiner, P., and Hüfner, S., 1974, *Phys. Rev.* B, **10,** 4038.
[51] Triplett, B. B., and Phillips, N. E., 1971, *Phys. Rev. Lett.*, **27,** 1001.
[52] Triplett, B. B., and Phillips, N. E., 1971, *Proceedings of the 12th International Conference on Low Temperature Physics*, edited by E. Kanda (Academic Press of Japan, Keigaku Publ. Co.,), p. 747.
[53] Steiner, P., Hüfner, S., and Zdrojewski, W. v., 1974, *Phys. Rev.* B, **10,** 4704.
[54] Frankel, R. B., Blum, N. A., Schwartz, B. B., and Kim, D. J., 1967, *Phys. Rev. Lett.*, **18,** 1051.
[55] Star, W. M., Basters, F. B., Nap, G. M., de Vroede, E., and van Baarle, C., 1972, *Physica*, **58,** 585.
[56] Doniach, S., 1977, *Physica* B, **91,** 231.
[57] Steiner, P., and Hüfner, S., 1975, *Phys. Rev.* B, **12,** 842.
[58] Riegel, D., Büermann, L., Gross, K. D., Luszik-Bhadra, M., and Mishra, S. N., 1988, *Phys. Rev. Lett.*, **61,** 2129; 1989, *Ibid.*, **62,** 316.
[59] Daybell, M. D., and Steyert, W. A., 1968, *Rev. mod. Phys.*, **40,** 380; Daybell, M. D., Pratt, Jr. W. P., and Steyert, W. A., 1969, *Phys. Rev. Lett.*, **22,** 401.
[60] Impens, G., and Dupré, A., 1980, *J. Magn. magn. Mater.*, **15–18,** 81.
[61] Vochten, M., Labro, M., and Vynckier, S., 1977, *Physica* B, **86–88,** 467.
[62] Daybell, M. D., and Steyert, W. A., 1968, *Phys. Rev. Lett.*, **20,** 195.
[63] Kondo, J., 1964, *Prog. theor. Phys.*, **32,** 37.
[64] Affleck, I., and Ludwig, A. W. W., 1991, *Nucl. Phys.* B, **360,** 641.
[65] Sacramento, P. D., and Schlottmann, P., 1989, *Phys. Lett.* A, **142,** 245; 1990, *Physica* B, **163,** 231. Due to numerical inaccuracy $S(T\rightarrow 0, H\neq 0)$ was incorrectly reported to be small but finite.
[66] Pang, H. B., and Cox, D. L., 1991, *Phys. Rev.* B, **44,** 9454.

[67] AFFLECK, I., LUDWIG, A. W. W., PANG, H. B., and COX, D. L., 1992, *Phys. Rev.* B, **45,** 7918.
[68] EMERY, V. J., and KIVELSON, S., 1992, *Phys. Rev.* B, **46,** 10812.
[69] GAN, J., ANDREI, N., and COLEMAN, P., 1993, *Phys. Rev. Lett.*, **70,** 686.
[70] SACRAMENTO, P. D., and SCHLOTTMANN, P., 1991, *J. appl. Phys.*, **70,** 5806.
[71] FULDE, P., and LOEWENHAUPT, M., 1986, *Adv. Phys.*, **34,** 589.
[72] OTT, H. R., RUDIGIER, H., FISK, Z., and SMITH, J. L., 1983, *Phys. Rev. Lett.*, **50,** 1595.
[73] STEWART, G. R., 1984, *Rev. mod. Phys.*, **56,** 755.
[74] OTT, H. R., RUDIGIER, H., FISK, Z., and SMITH, J. L., 1984, *Moment Formation in Solids*, edited by W. J. L. Buyers (Plenum, New York), p. 305.
[75] SHAPIRO, S. M., GOLDMAN, A. I., SHIRANE, G., COX, D. E., FISK, Z., and SMITH, J. L., 1985, *J. Magn. magn. Mater.*, **52,** 418.
[76] COX, D. L., 1987, *Theoretical and Experimental Aspects of Valence Fluctuations and Heavy Fermions*, edited by L. C. Gupta and S. K. Malik (Plenum, New York), p. 553.
[77] COX, D. L., 1988, *J. Magn. magn. Mater.*, **76&77,** 53.
[78] COX, D. L., 1988, *Physica* C, **153,** 1642.
[79] INGERSENT, K., JONES, B. A., and WILKINS, J. W., 1992, *Phys. Rev. Lett.*, **69,** 2594.
[80] SEAMAN, C. L., MAPLE, M. B., LEE, B. W., GHARNATY, S., TORIKECHVILI, M. S., KANG, J.-S., LIU, L. Z., ALLEN, J. W., and COX, D. L., 1991, *Phys. Rev. Lett.*, **67,** 2882.
[81] ANDRAKA, B., and TSVELIK, A. M., 1991, *Phys. Rev. Lett.*, **67,** 2886.
[82] LUDWIG, A. W. W., and AFFLECK, I., 1991, *Phys. Rev. Lett.*, **67,** 3160.
[83] TSVELIK, A. M., 1990, *J. Phys. Condensed Mater*, **2,** 2833.
[84] COX, D. L., unpublished, quoted as reference 20 in [82].
[85] AMITSUKA, H., HIDANO, T., HONMA, T., MITAMURA, H., and SAKAKIBARA, T., 1993, *Physica* B, **186–188,** 337.
[86] ANDRAKA, B., private communication.
[87] CALDEIRA, A. O., and LEGGETT, A. J., 1981, *Phys. Rev. Lett.*, **46,** 211; 1983, *Ann. Phys. (N.Y.)*, **149,** 374.
[88] BLACK, J. L., 1981, *Glassy Metals I*, edited by H. J. Güntherodt and H. Beck (Springer-Verlag, Berlin), p. 167.
[89] CHAKRAVARTY, S., and LEGGETT, A. J., 1984, *Phys. Rev. Lett.*, **52,** 5; BRAY, A., and MOORE, M. A., 1984, *Ibid.*, **49,** 1545.
[90] LEGGETT, A. J., CHAKRAVARTY, S., DORSEY, A. T., FISHER, M. P., GARG, A., and ZWERGER, W., 1987, *Rev. mod. Phys.*, **59,** 1.
[91] KONDO, J., 1976, *Physica* B, **84,** 40; 1976, *Ibid.*, **84,** 207.
[92] VLÀDAR, K., and ZAWADOWSKI, A., 1983, *Phys. Rev.* B, **28,** 1564; 1983, *Ibid.*, **28,** 1582; 1983, *Ibid.*, **28,** 1596.
[93] NOZIÈRES, P., and de DOMINICIS, C. T., 1969, *Phys. Rev.*, **178,** 1097.
[94] GOLDING, B., GRAEBNER, J. E., KANE, A. B., and BLACK, J. L., 1978, *Phys. Rev. Lett.*, **41,** 1487.
[95] DOUSSINEAU, P., 1981, *J. Phys., Paris, Lett.*, **42,** L83.
[96] ARNOLD, W., DOUSSINEAU, P., FRÈNOIS, CH., and LEVELUT, A., 1981, *J. Phys., Paris, Lett.*, **42,** L289.
[97] WEISS, G., HUNKLINGER, S., and von LÖHNEYSEN, H., 1981, *Phys. Lett.* A, **85,** 84; 1982, *Physica* B, **109&110,** 1946.
[98] WIPF, H., and NEUMAIER, K., 1984, *Phys. Rev. Lett.*, **52,** 1308; WANG, J. L., WEISS, G., WIPF, H., and MAGERL, A., 1984, *Phonon Scattering in Condensed Matter*, edited by W. Eisenmenger, K. Labmann and S. Dottinger (Springer-Verlag, Berlin), p. 401.
[99] YU, C. C., and ANDERSON, P. W., 1984, *Phys. Rev.* B, **29,** 6165.
[100] BLACK, J. L., VLÀDAR, K., and ZAWADOWSKI, A., 1982, *Phys. Rev.* B, **26,** 1559.
[101] VLÀDAR, K., ZIMÀNYI, G. T., and ZAWADOWSKI, A., 1986, *Phys. Rev. Lett.*, **56,** 286.
[102] RALPH, D. C., and BUHRMAN, R. A., 1992, *Phys. Rev. Lett.*, **69,** 2118.
[103] TAKANO, S., KUMASHIRO, Y., TSUJI, K., 1984, *J. Phys. Soc. Japan*, **53,** 4309.
[104] ISHIGURO, T., KANEKO, H., NOGAMI, Y., ISHIMOTO, H., NISHIYAMA, H., TSUKAMOTO, J., TAKAHASHI, A., YAMAURA, M., HAGIWARA, T., and SATO, K., 1992, *Phys. Rev. Lett.*, **69,** 660.
[105] BETHE, H. A., 1931, *Z. Phys.*, **71,** 205.
[106] ORBACH, R., 1958, *Phys. Rev.*, **112,** 309.
[107] SUTHERLAND, B., 1975, *Phys. Rev.* B, **12,** 3795.
[108] ANDREI, N., and JOHANNESSON, H., 1984, *Phys. Lett.* A, **100,** 108.

[109] LEE, K., and SCHLOTTMANN, P., 1988, *Phys. Rev.* B, **37,** 379.
[110] SCHLOTTMANN, P., and LEE, K., 1990, *Magnetic Properties of Low-Dimensional Systems II*, edited by L. M. Falicov, F. Mejía-Lira and J. L. Morán-López (Heidelberg: Springer-Verlag), p. 205.
[111] SACRAMENTO, P. D., 1993, *J. Phys. Condensed Matter*, **5,** 6999.
[112] LEE, K., and SCHLOTTMANN, P., 1989, *J. Phys. Condensed Matter*, **1,** 2759.
[113] LEE, K., and SCHLOTTMANN, P., 1987, *Phys. Rev.* B, **36,** 466.
[114] EGGERT, S., and AFFLECK, I., 1992, *Phys. Rev.* B, **46,** 10866.
[115] SORENSEN, E. S., EGGERT, S., and AFFLECK, I., preprint.
[116] SCHLOTTMANN, P., 1994, *Phys. Rev.* B, **49,** (in press).
[117] TSVELICK, A. M., unpublished.
[118] de VEGA, H. J., and WOYNAROVICH, F., 1992, *J. Phys.* A, **25,** 4499.
[119] CRAGG, D. M., and LLOYD, P., 1979, *J. Phys.* C, **12,** 3301; CRAGG, D. M., LLOYD, P., and NOZIÈRES P., 1980, *J. Phys.* C, **13,** 803.
[120] ABRIKOSOV, A. A., and MIGDAL, A. A., 1970, *J. Low Temp. Phys.*, **3,** 519.
[121] See e.g. COX, D. L., JARRELL, M., JAYAPRAKASH, C., KRISHNA-MURTHY, H. R., and DEISZ, J., 1989, *Phys. Rev. Lett.*, **62,** 2188.
[122] JONES, B. A., and VARMA, C. M., 1987, *Phys. Rev. Lett.*, **58,** 843.
[123] JAYAPRAKASH, C., KRISHNA-MURTHY, H. R., and WILKINS, J. W., 1981, *Phys. Rev. Lett.*, **47,** 737.
[124] JONES, B. A., VARMA, C. M., and WILKINS, J. W., 1989, *Phys. Rev. Lett.*, **61,** 125.
[125] HALDANE, F. D. M., 1977, *Phys. Rev.* B, **15,** 2477.
[126] PERAKIS, I. E., VARMA, C. M., and RUCKENSTEIN, A. E., 1993, *Phys. Rev. Lett.*, **70,** 3467.
[127] GIAMARCHI, T., VARMA, C. M., RUCKENSTEIN, A. E., and NOZIÈRES, P., 1993, *Phys. Rev. Lett.*, **70,** 3967.
[128] SCHLOTTMANN, P., 1993, *Phys. Rev. Lett.*, **68,** 1916.
[129] SCHLOTTMANN, P., 1994, *Phys. Rev.* B, **49** (in press).